AD-A154 816   THE STUDY OF WHITE-LIGHT OPTICAL IMAGE SUBTRACTION FOR   1/ℓ
                POSSIBLE APPLICATI..(U) PENNSYLVANIA STATE UNIV
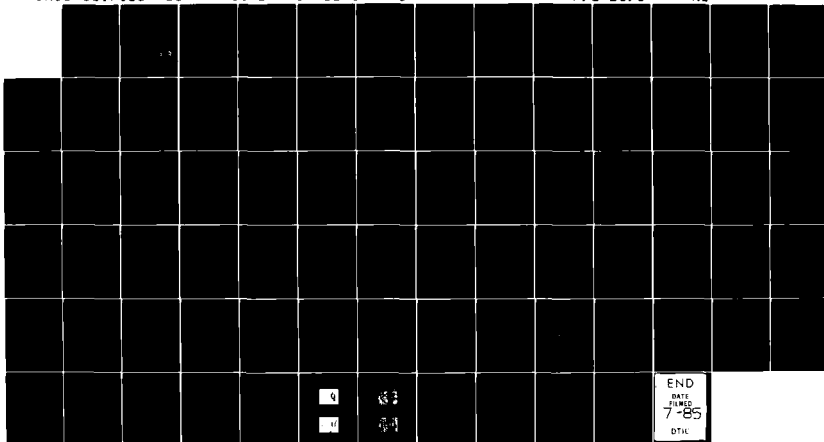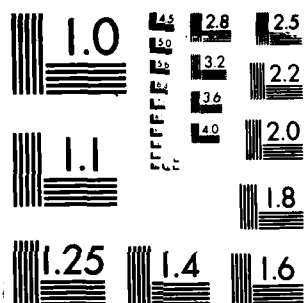   UNIVERSITY PARK DEPT OF ELECTRICAL EN.. F T YU
UNCLASSIFIED   25 MAR 83 DAAH01-82-C-A142   F/G 20/6   NL

MICROCOPY RESOLUTION TEST CHART

NATIONAL BUREAU OF STANDARDS 1963 A

The Study of White-Light Optical Image Subtraction
for Possible Application to Missile
Tracking and Identification

Final Report
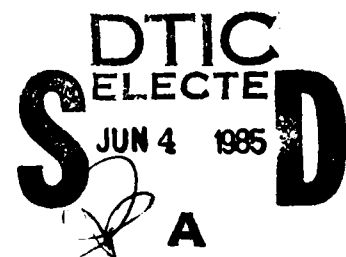
Contract No. DAAH01-82-C-A142

Prepared by:

F. T. S. Yu

Electrical Engineering Department
The Pennsylvania State University
University Park, PA 16802

For:

U.S. Army Missile Laboratory
U.S. Army Missile Command
Redstone Arsenal, AL 35898

Attention: DRSMI-RRO
Dr. J. Graeme Duthie

Period Covered (February 19, 1982 - February 18, 1983)

Date: March 25, 1983

REPORT DOCUMENTATION PAGE	READ INSTRUCTIONS BEFORE COMPLETING FORM

1. REPORT NUMBER	2. GOVT ACCESSION NO.	3. RECIPIENT'S CATALOG NUMBER
	AD-A154 816	

4. TITLE (and Subtitle)	5. TYPE OF REPORT & PERIOD COVERED
The study of white-light optical image subtraction for possible application to missile tracking and identification	Final Technical Report
	6. PERFORMING ORG. REPORT NUMBER

7. AUTHOR(s)	8. CONTRACT OR GRANT NUMBER(s)
Francis T.S. Yu	DAAH01-82-C-A142

9. PERFORMING ORGANIZATION NAME AND ADDRESS	10. PROGRAM ELEMENT, PROJECT, TASK AREA & WORK UNIT NUMBERS
Electrical Engineering Department The Pennsylvania State University University Park, PA 16802	

11. CONTROLLING OFFICE NAME AND ADDRESS	12. REPORT DATE
Dr. J. Graeme Duch U.S. Army Missile Command, DRSMI-RRO Redstone Arsenal, AL 35898	March 25, 1983
	13. NUMBER OF PAGES 71

14. MONITORING AGENCY NAME & ADDRESS (if different from Controlling Office)	15. SECURITY CLASS. (of this report)
	Unclassified
	15a. DECLASSIFICATION DOWNGRADING SCHEDULE

16. DISTRIBUTION STATEMENT (of this Report)

This document has been approved for public release and sale; its distribution is unlimited.

17. DISTRIBUTION STATEMENT (of the abstract entered in Block 20, if different from Report)

18. SUPPLEMENTARY NOTES

19. KEY WORDS (Continue on reverse side if necessary and identify by block number)

Optical signal processor, image subtraction, white-light optical processing, missile tracking and identification, optical signal detection.

20. ABSTRACT (Continue on reverse side if necessary and identify by block number)

In this study, the coherence requirement for an incoherent image subtraction processor is analyzed, with the partial coherence theory of Wolf. We have shown that image subtraction operation is basically a 1-D processing operation and the spatial coherence requirement is a point pair concept. A source encoding mask can be utilized to alleviate the constraint of a physical light source, such that the image subtraction can be carried out with extended incoherent source.

DD FORM 1473 EDITION OF 1 NOV 65 IS OBSOLETE
1 JAN 73

85 5 13 111

20. ABSTRACT *(Continued)*

We have also in this study demonstrated the possibility of utilizing the image subtraction technique as applied to micro-circuit board inspection, which would have a profound effect on precision inspection scheme for large scale automatic assembly for U.S. Army needs and her supporting industries. This technique would provide the capability of rapid identification inspection, and possibly utilizing for synthesis and fabrication. The effects due to coherence requirement are also included. Experimental simulations of the IC chip inspection are provided.

We have also reported an application of this source encoding technique to generate a 2-D color hologram with an extended incoherent source. The color hologram image can be retrieved with a simple white-light optical processor. Experimental demonstration of a color hologram image generated by this technique is included. We have noted that a 3-D hologram image for phase-type object of definite depth may be generated by this technique.

Finally, the net effect is to emphasize the truth of our initial assumption of the white-light image subtraction can be an essential part of the missile tracking and identification application. This research effort in real-time tracking program should be continuing to pursue.

Accession For

NTIS GRA&I

DTIC TAB

Unannounced

Justification

By

Distribution

Availability Codes

Dist   Special

A-1

Table of Contents

List of Illustrations

List of Tables

I.   Introduction

1.1   U.S. Army Goals and Needs

The U.S. Army needs to improve the tracking technology not only by improving the simplicity of the tracking equipment but also needs to improve the quality and versatility of the technique.

The basic tracking technique that we would like to investigate may center at white-light optical image subtraction technique; particularly in the application to missile tracking and identification. We would like to stress that the image subtraction technique, as compared with the optical correlation detection technique[1], in the application to missile tracking offers the following advantages:

1. The tracking technique is generally free from scale and object orientation problems.

2. The system is not limited to a small number of objects to be detected.

3. Since the system does not employ matched spatial filter, the tracking system is versatile and simpler to operate.

4. The system is generally smaller and economical to install.

There are also several reasons for selecting the optical image subtraction technique rather than their electronic or digital counterpart, because the optical technique has the following capabilities:

1. It is capable of handling very large information elements.

2. It has a very large space-bandwidth product.

3. It has the capability of performing parallel

tracking and identification.

4. The compatibility with optical storage techniques.

We would, however, use the white-light or incoherent source

rather than the coherent optical counterpart, because of the

following advantages:

1. It eliminates the coherent artifact noise that

generally plagues the coherent optical system.

2. The white-light tracking system is generally

economical to operate and easy to maintain.

3. The white-light technique is very versatile and

simpler to handle.

4. The white-light system is generally not sensitive

to vibrational problem.

5. The white-light tracking system is relatively

smaller and simpler to install.

We emphasize again, the basic objective of this proposed

research is to improve the tracking and identification capa-

bilities so that reliable tracking signals can be obtained.

1.2 Image Subtraction with Extended Incoherent Source

We shall in this section describe a source encoding tech-

nique for incoherent image subtraction. We note that this

source encoding techique is capable of reducing the spatial

coherent requirement of the light source for image subtraction

and at the same time suppresses the coherent artifact noise of

the processing system. In other words, the incoherent image

subtraction system is capable of subtracting the images in compex amplitude like a coherent processor, and at the same time it suppresses the coherent artifact noise like an incoherent processor.

Since the image subtraction problem is essentially a one-dimensional processing problem, a very narrow slit incoherent light source can be utilized. Since the spatial coherent requirement for image subtraction is only required at every corresponding image points between the two images, therefore only a point-pair spatial coherence between the two images is required. In order to obtain a point-pair spatial coherence over the input plane P_2 of an incoherent processor of Fig. 1-1, we would encode the extended source with a set of narrow slit apertures over the source plane P_1. Now with reference to Fig. 1-1 and the use of the Van Cittert-Zernike's theory[2], the degree of spatial coherent over the input plane P_2 of the incoherent optical processor can be shown[3-4].

$$\mu(x_1 - x_2) = \frac{\mathrm{Sin}\left(2N\pi \, \frac{x_1 - x_2}{2h_o}\right)}{N \, \mathrm{Sin}\left(2\pi \, \frac{x_1 - x_2}{2h_o}\right)} \quad X \quad \frac{\mathrm{Sin} \, 2\pi \, \frac{s(x_1 - x_2)}{h_o d}}{2\pi \, \frac{s(x_1 - x_2)}{h_o d}}, \quad (1-1)$$

where d is the spacing of the slits, s is the slit width, and N is the total number of slits over the extended source. From the above equation we see that the degree of spatial coherence for each pair of points between the two images over the input plane P_2 separated by a distance $2h_o$ can be shown equals to[3-4]

$$\mu(2h_o) = \mathrm{Sinc}\left(\frac{2 \cdot s}{d}\right). \quad (1-2)$$
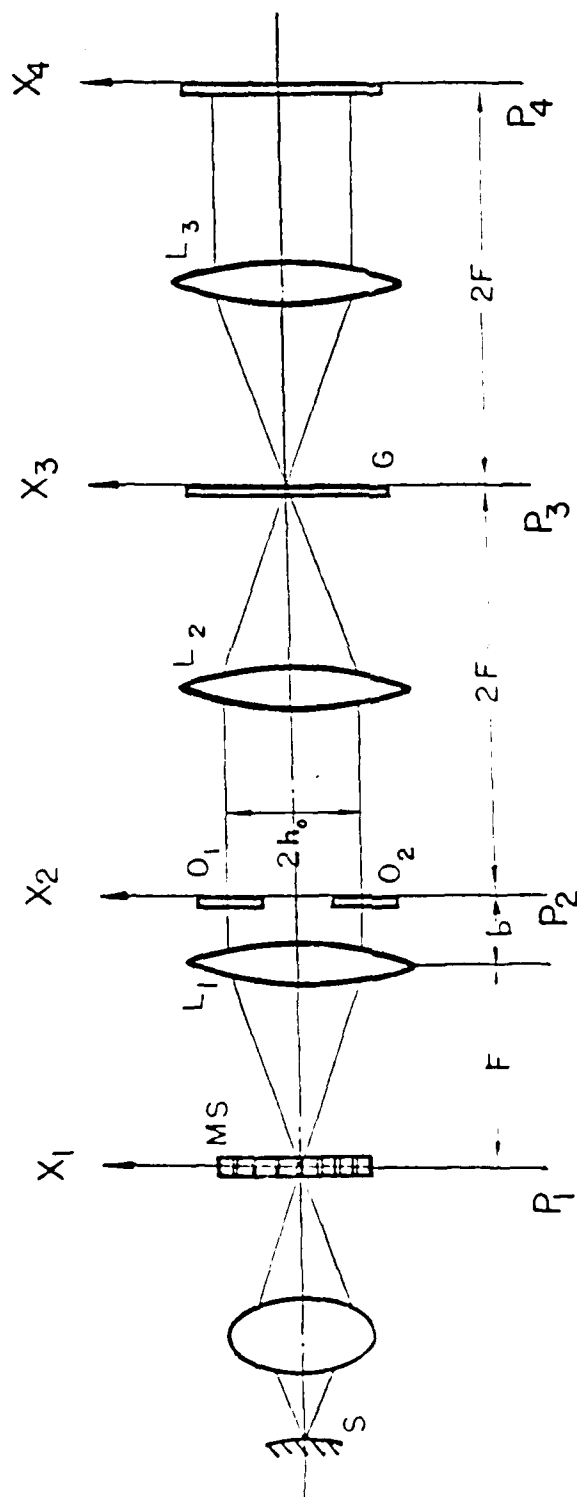
Figure 1-1.   Image Subtraction With Extended Incoherent
Source. S; Mercury Arc Lamp, MS; Multi-
slit Mask, O_1 and O_2, Object Trans-
parencies, G: Grating.

Thus for $\frac{s}{d} \ll 1$, a high degree of spatial coherence between
the corresponding image points can be obtained, and a brighter
subtracted image can be observed at the output plane P_4 of
the processor. We see that the incoherent processor is indeed
capable of processing the image in complex amplitude like a
coherent processor. In comparison with a single slit case[5],
the intensity of the output image in increased N fold, so
that the output subtracted image can be made observable. We
would note that the basic objective of source encoding is
to provide an appropriate coherent requirement for certain
optical information processing operation such that more
efficient utilization of source power can be achieved.

We would also note that the source encoding technique can
be extended for extended white-light source, a research program
is currently still pursuing. In addition, pseudocolor encoding
technique can also be implemented for image subtraction for
target tracking position. In other words, it is possible to
deplay the subtracted image (i.e., target) in one color super-
imposed with the background in another color.

Although the proposed incoherent image subtraction tech-
nique is aiming at the application to missile tracking and
identification, there are several other areas of intense interest
to the U.S. Government relying on signal tracking technology
and hence it stands to benefit from our research work. Those
areas are radar, sonar, etc.

1.3 Report Outline

We deal primarily on an image subtraction with incoherent
source as applied to tracking and identification. Since the

the output plsne P_3 will be searched for, that is

$$J(x_1',y_1';x_2',y_2';\lambda)=\iiint J'(x_1,y_1;x_2,y_2;\lambda)\exp\{-j\frac{2\pi}{\lambda f}(x_1'\alpha_1+y_1'\beta_1$$

$$-x_2'\alpha_2-y_2'\beta_2)\}d\alpha_1 d\beta_1 d\alpha_2 d\beta_2 \quad . \tag{2-19}$$

Basic interest is usually centered on the output intensity distribution $I(x'',y'';\lambda)$; by letting $x_1''=x_2''=x''$ and $y_1''=y_2''=y''$ Eq.(2-19) can be written as

$$I(x',y';\lambda)=\iint \gamma(x_o,y_o;\lambda)dx_o dy_o\iint S(x_o+\alpha_1-\lambda f y_o,y_o+\beta_1)H(\alpha_1,\beta_1)$$

$$\times \exp\{-j\frac{2\pi}{\lambda f}(\alpha_1 x'+\beta_1 y')\}d\alpha_1 d\beta_1\iint S^*(x_o+\alpha_2-\lambda f y_o,y_o+\beta_2)$$

$$\times H^*(\alpha_2,\beta_2)\exp\{j\frac{2\pi}{\lambda f}(\alpha_2 x'+\beta_2 y')\}d\alpha_2 d\beta_2 \quad . \tag{2-20}$$

By interchanging the variables (α_1,β_1) and (α_2,β_2) to (α,β), Eq.(2-20) reduces to

$$I(x',y';\lambda)=\iint \gamma(x_o,y_o;\lambda)|\iint S(x_0+\alpha-\lambda f y_o,y_o+\beta)H(\alpha,\beta)$$

$$\times \exp\{-j\frac{2\pi}{\lambda f}(\alpha x'+\beta y')\}d\alpha d\beta|^2 dx_o dy_o \quad , \tag{2-21}$$

We define $S(\lambda)$ as the relative spectral intensity of the light source and $C(\lambda)$ as the relative spectral response sensitivity of the detector or recording material. Since the different wavelengths of the light source are

$$J(\alpha_1,\beta_1;\alpha_2,\beta_2;\lambda)=\iint\gamma(x_o,y_o;\lambda)[S(x_o+\alpha_1,y_o+\beta_1)+\tfrac{1}{2}S(x_o+\alpha_1-\lambda f\nu_o,y_o+\beta_1)$$

$$+\tfrac{1}{2}S(x_o+\alpha_1+\lambda f\nu_o,y_o+\beta_1)][S^*(x_o+\alpha_2,y_o+\beta_2)+\tfrac{1}{2}S^*(x_o+\alpha_2$$

$$+\lambda f\nu_o,y_o+\beta_2)+\tfrac{1}{2}S^*(x_o+\alpha_2-\lambda f\nu_o,y_o+\beta_2)]dx_o dy_o \quad,$$

$$(2\text{-}15)$$

where the integration is over the source plane P_o, and $S(\alpha,\beta)$ is the Fourier spectrum of the input $s(x,y)$ i.e.,

$$S(\alpha,\beta)=F\{s(x,y)\} \quad . \qquad (2\text{-}16)$$

If the complex transmittance of the spatial filter at the Fourier plane is equal to $H(\alpha,\beta)$, the mutual intensity function immediately behind the spatial filter will be

$$J'(\alpha_1,\beta_1;\alpha_2,\beta_2;\lambda)=J(\alpha_1,\beta_1;\alpha_2,\beta_2;\lambda)H(\alpha_1,\beta_1)H^*(\alpha_2,\beta_2) \quad . \qquad (2\text{-}17)$$

For convenience, assume that the spatial filter is only effective over one of the smeared Fourier spectra; then Eq.(2-15) becomes

$$J'(\alpha_1,\beta_1;\alpha_2,\beta_2;\lambda)=\iint\gamma(x_o,y_o;\lambda)S(x_o+\alpha_1-\lambda f\nu_o,y_o+\beta_1)S^*(x_o+\alpha_2-\lambda f\nu_o,$$

$$y_o+\beta_2)H(\alpha_1,\beta_1)H^*(\alpha_2,\beta_2)dx_o dy_o \quad, \qquad (2\text{-}18)$$

where the appropriate constant has been ignored.

In the final step, the mutual intensity function at

For simplicity, assume that the achromatic lenses are infinitely extended. By Eq.(2-11), the mutual intensity function at the input plane P_1 due to the source intensity distribution $\Upsilon(x_0,y_0)$ for every wavelength can be written

$$J(x_1,y_1;x_2,y_2;\lambda)=\iint\Upsilon(x_0,y_0;\lambda)\exp\{-j\frac{2\pi}{\lambda f}[(x_1-x_2)x_0+(y_1-y_2)y_0]\}dx_0dy_0 \quad .$$

$$(2-12)$$

where (x_1,y_1) and (x_2,y_2) are two arbitrary points over the input plane (x,y), f is the focal length of the achromatic transform lens, and the integration is over the source plane P_0. The mutual intensity function immediately behind the diffraction grating G can be written

$$J'(x_1y_1;x_2,y_2;\lambda)=J(x_1,y_1;x_2,y_2;\lambda)s(x_1,y_1)s^*(x_2,y_2)$$

$$x[1+\cos(2\pi\nu_0x_1)][1+\cos(2\pi\nu_0x_2)] \quad , \qquad (2-13)$$

where the superscript denotes the complex conjugate, and ν_0 is the spatial frequency of the diffraction grating. Similarly, the mutual intensity function at the Fourier plane P_2 can be written

$$J(\alpha_1,\beta_1;\alpha_2,\beta_2;\lambda)=\iiiint J'(x_1,y_1;x_2,y_2;\lambda)\exp\{-j\frac{2\pi}{\lambda f}[\alpha_1x_1+\beta_1y_1$$

$$-\alpha_2x_2-\beta_2y_2]\}dx_1dy_1dx_2dy_2 \quad ; \qquad (2-14)$$

where the integration is over the input plane P_1. By substituting Eqs.(2-12) and (2-13) into Eq.(2-14), we have
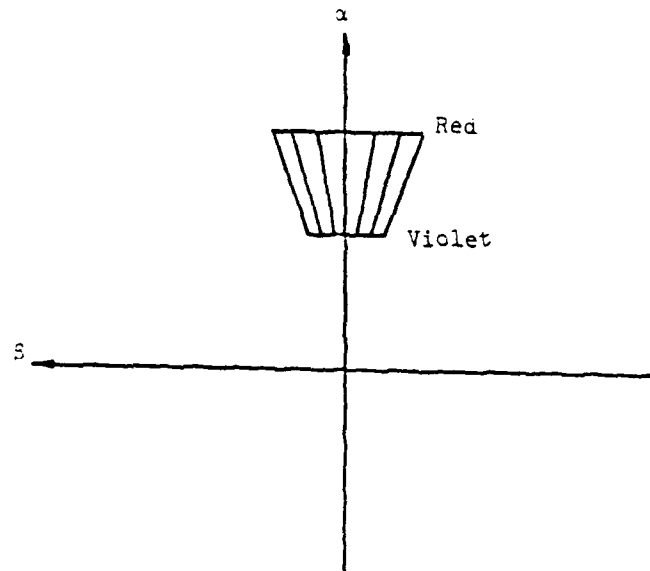
Figure 2-2. Fan Shape Filter for One-Dimensional Operation.
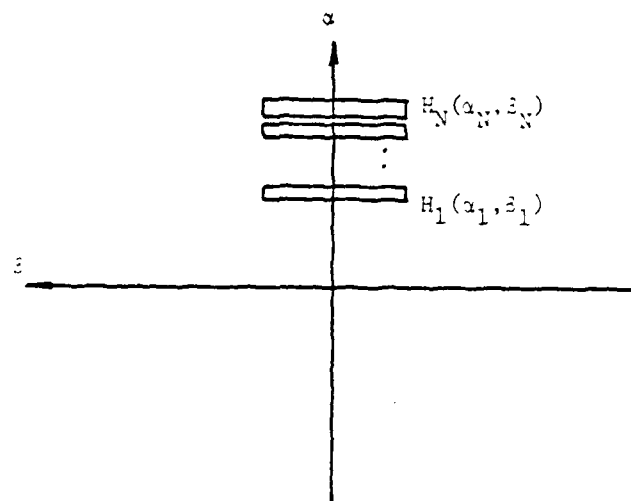
Figure 2-3. Multi-Narrow Band Filter for Two-Dimensional Operation.

Consider the partially coherent optical processing system, which was proposed by Yu[13,16,17] diagrammed in Fig.1-3. Due to the diffraction grating the spectrum of the input signal will disperse into rainbow colors in the Fourier plane P_2 achieving higher temporal coherence along the α-direction. Therefore, the input signal $s(x,y)$ can be processed in complex amplitude. If the processing operation is one-dimensional, a fan-shaped spatial filter, which is shown in Fig.2-2, can be used to accommodate the wavelength variation. For a two-dimensional processing operation a set of narrow strip filters $H_n(\alpha_n, \beta_n)$, $(n=1,2,\ldots\ldots n)$, can be used to process different color signals band by band as shown in Fig.2-3 Each of the spatial filters is synthesized for a narrow spectral band, for which the center wavelength is λ_{on} and the bandwidth is equal to $\Delta\lambda_n$. The filtered signal will be incoherently superimposed at output plane P_3.

The calculation of the intensity distribution at the output plane may be divided into three steps as follows

(1) Derive the output mutual intensity function for a single wavelength λ_{on}.

(2) Calculate the output intensity distribution $I_n(x',y')$, which is related to the narrow strip spatial filter.

(3) Add $I_n(x',y')$ (n through 1 to N) to obtain the total output intensity distribution $I(x',y')$.

where $\gamma\,(x_o,y_o)$ is the intensity distribution of the incoherent light source, and (x_o,y_o) is the coordinate of the light source plane. In this case the mutual intensity function at the input plane is simply equal to

$$J_1(x_1-x_2;y_1-y_2)=\int\!\!\int_\infty^\infty \gamma(x_o,y_o)\exp\{-j\frac{k}{2f}[(x_1-x_2)x_o+(y_1-y_2)y_o]\}dx_ody_o \quad .$$

(2-11)

It is evident from Eq.(2-11) that the mutual intensity function at the input plane, illuminated by an extended incoherent source, is a space invariant function.

2.3 General Formula for a Partially Coherent Optical Processor

An optical information processing operation under the partially coherent regime will now be described. The optical processing operation depends on the degree of spatial and temporal coherence for the source, as do the spatial frequency response (i.e.,transfer function) and the noise performance of the optical processor. We will investigate the coherence requirements, of a general and specific optical processor. We will look into the effects of the size and the spectral bandwidth of the light source employed on the intensity distribution at the output plane.

Thus the mutual intensity function of the light at the point pair (α_1, β_1) and (α_2, β_2) is related to the Fourier spectrum of the mutual intensity at the input plane. We note that the Fourier transform relation between the input and the focal plane for the mutual intensity function is not an exact one, due to the presence of the quadratic phase factor that precedes the four-dimensional integral.

(b) If we let d_o be equal to f, the quadratic phase factor vanishes and Eq.(2-8) could be again simplified as

$$J_4(\alpha_1,\beta_1;\alpha_2,\beta_2)=C\iiiint_{-\infty}^{\infty} J_1(x_1,y_1;x_2,y_2)\exp\{-j\frac{k}{2f}[(\alpha_1 x_1+\beta_1 y_1)$$

$$-(\alpha_2 x_2+\beta_2 y_2)]\}dx_1 dy_1 dx_2 dy_2 \quad . \qquad (2-9)$$

Evidently when the input is placed in the front focal plane of an ideal thin lens, an exact four-dimensional Fourier transform relation can be obtained for the mutual intensity function.

(c) In partially coherent optical processing an extended incoherent light source is usually placed at the front focal plane of the collimation lens to illuminate the input transparency, which is inserted in the back focal plane of the collimator. Then

$$J(\overline{x}_1,\overline{y}_1;\overline{x}_2,\overline{y}_2)= \begin{cases} \gamma(x_o,y_o) \quad , & \text{for } \overline{x}_1=\overline{x}_2=x_o \ , \ \overline{y}_1=\overline{y}_2=y_o \ , \\ 0 & \text{otherwise} \quad , \end{cases} \qquad (2-10)$$

wher$\cdot$ c is a constant.

Eq.(2-7) illustrates that the mutual intensity of the light at the output plane could be calculated by a four-dimensional integration.

To this point we have entirely neglected the finite extent of the lens aperture. We note that such an approximation is an accurate one if the distance d_o is sufficiently small to place the input deep within the region of Fresnel diffraction for the lens aperture. This condition is satisfied in the vast majority of problems of interest. The limitation of the effective input by the finite lens aperture is known as a ´vignetting´ effect. Note that vignetting in the input space is minimized when the input is placed close to the lens and when the lens aperture is much larger than the input. In practice it is often preferred to place the object directly against the lens in order to minimize vignetting.

There are three particular cases of the general formula (2-7) worth mentioning:

(a) For the case that $d_1 = f$, the output is placed at the back focal plane. Eq.(2-7) becomes

$$J_4(\alpha_1, \beta_1; \alpha_2, \beta_2) = C \ \exp\{j\frac{k}{2f}(1 - \frac{d_o}{f})[(\alpha_1^2 + \beta_1^2) - (\alpha_2^2 + \beta_2^2)]\}$$

$$\times \int\!\!\int\!\!\int\!\!\int_{-\infty}^{\infty} J_1(x_1, y_1; x_2, y_2) \exp\{-j\frac{k}{2f}[(\alpha_1 x_1 + \beta_1 y_1) - (\alpha_2 x_2 + \beta_2 y_2)]\} \ dx_1 dy_1 dx_2 dy_2 .$$

$$x \; (\xi_1^2 + \eta_1^2 - \xi_2^2 - \eta_2^2) - 2\xi_1 (\frac{\alpha_1}{d_1} + \frac{x_1}{d_o}) - 2\eta_1 (\frac{\beta_1}{d_1} + \frac{y_1}{d_o}) + 2\xi_2 (\frac{\alpha_2}{d_1} + \frac{x_2}{d_o})$$

$$+ 2\eta_2 (\frac{\beta_2}{d_1} + \frac{y_2}{d_o})] \} \, d\xi_1 d\eta_1 d\xi_2 d\eta_2] dx_1 dy_1 dx_2 dy_2 \qquad ; \qquad (2\text{-}5)$$

note that

$$\int_{-\infty}^{\infty} \exp \{ jk [(\frac{1}{d_1} + \frac{1}{d_0} - \frac{1}{f}) \xi_1^2 - 2\xi_1 (\frac{\alpha_1}{d_1} + \frac{x_1}{d_0})] \; d\xi_1 = \exp \{ -jk (\frac{\alpha_1}{d_1} + \frac{x_1}{d_o})$$

$$/ (\frac{1}{d_1} + \frac{1}{d_o} - \frac{1}{f}) \int_{\infty}^{\infty} \exp \{ jk (\frac{1}{d_1} + \frac{1}{d_o} - \frac{1}{f}) [\xi_1 - (\frac{\alpha_1}{d_1} + \frac{x_1}{d_o}) / (\frac{1}{d_1} + \frac{1}{d_o}$$

$$- \frac{1}{f})]^2 \} d\xi_1 = \frac{1}{2} [\frac{\pi}{jk (\frac{1}{d_1} + \frac{1}{d_o} - \frac{1}{f})}]^{\frac{1}{2}} \exp \{ -jk (\frac{1}{d_1} + \frac{x_1}{d_o})^2 / (\frac{1}{d_1} + \frac{1}{d_o} - \frac{1}{f}) \}$$

$$(2\text{-}6)$$

There are similar formulas for variables η_1, ξ_2 and η_2. Therefore the transformation formula for the mutual intensity function due to an ideal thin lens is

$$J_4 (\alpha_1, \beta_1; \alpha_2, \beta_2) = C \; \exp \{ j \frac{k}{2d_1} [1 - \frac{1}{d_1 (\frac{1}{d_1} + \frac{1}{d_o} - \frac{1}{f})}] [(\alpha_1^2 + \beta_1^2) - (\alpha_2^2 + \beta_2^2)] \}$$

$$x \int_{\infty}^{\infty} \!\!\! \int\!\!\int\!\!\int J_1 (x_1, y_1; x_2, y_2) \exp \{ j \frac{k}{2d_o} [1 - \frac{1}{d_o (\frac{1}{d_1} + \frac{1}{d_o} - \frac{1}{f})}] [(x_1^2 + y_1^2) - (x_2^2 + y_2^2)] \}$$

$$x \; \exp \{ -jk \frac{ (\xi_1 x_1 + \eta_1 y_1) - (\xi_2 x_2 + \eta_2 y_2) }{ d_o d_1 (\frac{1}{d_1} + \frac{1}{d_o} - \frac{1}{f}) } \} dx_1 dy_1 dx_2 dy_2 \qquad , \qquad (2\text{-}7)$$

$$J_2(\xi_1,\eta_1,\xi_2,\eta_2) = -\frac{1}{\lambda^2 d_o^2}\iiiint_{-\infty}^{\infty} J_1(x_1,y_1,x_2,y_2)\exp\{j\,\frac{k}{2d_o}$$

$$\times[(\xi_1-x_1)^2+(\eta_1-y_1)^2]\}\exp\{-j\frac{k}{2d_o}[(\xi_2-x_2)^2+(\eta_2-y_2)^2]\}\,dx_1 dy_1 dx_2 dy_2 \qquad , \tag{2-2}$$

and the mutual intensity function immediately behind the lens will be

$$J_3(\xi_1,\eta_1;\xi_2,\eta_2) = J_2(\xi_1,\eta_1;\xi_2,\eta_2)t_o(\xi_1,\eta_1)t_o^*(\xi_2,\eta_2) \qquad , \tag{2-3}$$

The superposition integral from plane (ξ,η) to plane (α,β) is

$$J_4(\alpha_1,\beta_1;\alpha_2,\beta_2) = -\frac{1}{\lambda^2 d_1^2}\iiiint_{\infty}^{\infty} J_3(\xi_1,\eta_1;\xi_2,\eta_2)\exp\{j\,\frac{k}{2d_1}[(\alpha_1-\xi_1)^2+(\beta_1-\eta_1)^2]\}$$

$$\times \exp\{-j\,\frac{k}{2d_1}[(\alpha_2-\xi_2)^2+(\beta_2-\eta_2)^2]\}\,d\xi_1 d\eta_1 d\xi_2 d\eta_2 \qquad . \tag{2-4}$$

Substituting Eqs. (2-1) and (2-3) into Eq. (2-4), we can express the mutual intensity function at the output plane as

$$J_4(\alpha_1,\beta_1;\alpha_2,\beta_2) = \frac{1}{4d_o^2 d_1^2}\exp\{j\frac{k}{d_1}(\alpha_1^2+\beta_1^2)-(\alpha_2^2+\beta_2^2)\}$$

$$\times \iiiint_{-\infty}^{\infty} J_1(x_1,y_1;x_2,y_2)\exp\{j\,\frac{k}{d_o}(x_1^2+y_1^2)-(x_2^2+y_2^2)\} \qquad .$$

$$\times[\iiiint_{-\infty}^{\infty}\exp\{jk(\frac{1}{d_1}+\frac{1}{d_o}-\frac{1}{f})$$
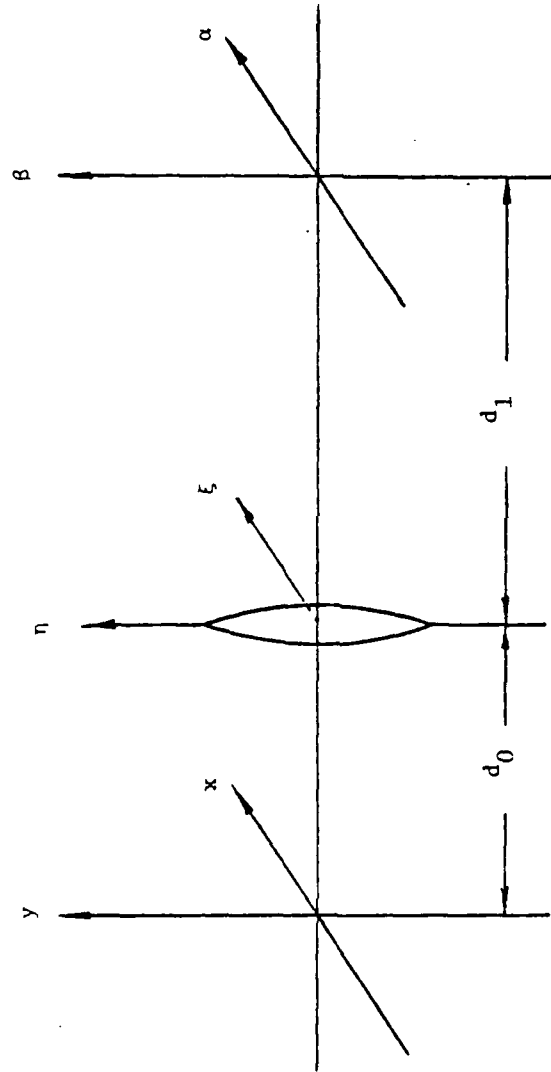
Fig.2-1. Fourier Transforming with Object Placed Behind the Lens.

dimensional Fourier transformation of a light signal in complex amplitune[14,15]. For partially coherent light we can show that the four-dimensional Fourier transformation of the mutual intensity function could be performed by an ideal thin lens.

It can be shown that a plane wave passing through a thin lens experiences a phase delay factor of $t_o(\xi,\eta)$ such as[15],

$$t_o(\xi,\eta) = \exp[jkn\Delta_o]\exp[-jk(\xi^2+\eta^2/2f],\qquad(2-1)$$

where n is the refractive index of the lens material, f is the focal length, Δ_o is the center thickness of the lens, $k = 2\pi/\lambda$, where λ is the wavelength of light, and (ξ,η) is the coordinate system of the lens plane. The first term of Eq. (2-1) is simply a constant phase delay, while the second term may be recognized as a quadratic phase factor associated with a spherical wave.

Consider the more general geometry of Fig. 2-1, where an object, located a distance d_o in front of the lens, is illuminated by spatially partial coherent light. If the mutual intensity function at the object plane is $J_1(x_1,y_1:x_2,y_2)$, our goal is to try to find the mutual intensity function at the output plane, which is behind the lens at distance d_1. The light at the lens plane (ξ,η) can be expressed by using the superposition integral

of correlation in an investigation relating to image formation for · microscope[3].

An important stage in the development of this subject was made by Van Cittert[9] and Zernike[10]. They determined the "degree of coherence" for the light disturbances at any two points on a screen illuminated by an extended primary source. The method was simplified further and applied to the study of image formation and resolving power by Hopkins[11]. Wolf introduced a correlation function, which was found to obey rigorously the wave equation, to depict the correlation proper-ties of the light disturbances at any two points[12]. Such 'second order' correlation functions are adequate for the analysis of the usual optical experiments involving interference and diffraction of light from steady sources.

Before investigating the behavior of a partially coherent optical processor, it is necessary to establish the transforma-tion relations of the mutual intensity function (or correlation function), which is equal to the degree of coherence in the image of an extended incoherent quasi-monochromatic illumination. In this section, we use Wolf's theory[12] of partially coherent light to develop a transformation formula for the mutual intensity function passing through an ideal thin lens. We then apply it to derive the general formula for the partially coherent optical processor which was introduced by Yu[13].

2.2 Propagation of Mutual Intensity Function

One of the most remarkable and useful properties of a converging lens is its inherent ability to perform the two-

image subtraction operation relies on complex amplitude opera-
tion, the partial coherent requirement of the extended source
image subtractor should be evaluated. The feasibility and the
constraints of the system performance should be discussed. We
shall report in the following the analysis of the coherence
requirement for the proposed incoherent image subtraction system.
The application of this proposed image subtraction system to
IC chip inspection are given. Experimental demonstrations for
the IC mask inspection is included. We shall also report a
technique of generating a 2-D color hologram with the image
subtraction technique. An experimental result of color holo-
gram image obtained with this proposed system is also provided.

II. Image Formation by Partially Coherent Illumination

2.1 Introduction

Researchers in optical information processing have confined
their attention to the analysis and synthesis of optical systems
in which the illumination is either extremely coherent or
incoherent. Surely we must expect a continuous transition
between these two extreme limits. Such a transitional region
exists and is known as the field of partial coherence.

The first investigation which has a close bearing on the
subject of partial coherence was done by Verdet, who studied
the size of the region of coherence for light from an extended
source[6]. Later, Michelson established the connection between
the visibility of interference fringes and the intensity dis-
tribution on the surface of an extended primary source[7]. A
further contribution was made by Berek, who used the concept

mutually incoherent, the intensity distribution related to
th narrow strip filter can be written as

$$I_n(x',y') = \int_{\lambda_{on}-\Delta\lambda_n/2}^{\lambda_{on}+\Delta\lambda_n/2} \iint_\infty^\infty \gamma(x_o,y_o;\lambda)S(\lambda)C(\lambda) \,|\iint_\infty S(x_o+\alpha-\lambda f\nu_o,y_o+\beta)$$

$$H(\alpha,\beta)\exp\{-j\frac{2\pi}{\lambda f}(x'\alpha+y'\beta)\}d\alpha d\beta|^2 dx_o dy_o d\lambda \quad , \qquad (2-22)$$

where λ_{on} is the center wavelength and $\Delta\lambda_n$ is the
bandwidth corresponding to the nth narrow strip filter.
Finally the overall intensity distribution, due entirely
to the spectral band of the light source, at the output
plane would be,

$$I(x',y') = \sum_{n=1}^N I_n(x',y')$$

$$= \sum_{n=1}^N \int_{\lambda_{on}-\Delta\lambda_n/2}^{\lambda_{on}+\Delta\lambda_n/2} \iint_\infty^\infty \gamma(x_o,y_o;\lambda)S(\lambda)C(\lambda) \,\iint_\infty^\infty S(x_o+\alpha-\lambda f\nu_o,y_o+\beta)$$

$$H(\alpha,\beta)\exp\{-j\frac{2\pi}{\lambda f}(x'\alpha+y'\beta)\}d\alpha d\beta|^2 dx_o dy_o d\lambda \quad . \qquad (2-23)$$

which is essentially the incoherent summation of the filtered
signals.

III. Coherence Requirement

3.1 Introduction

Since its invention, the laser has been a fashionable
tool for many applications, particularly for coherent optical

information processing. This trend is mainly due to the complex amplitude processing capabilities of the coherent light. Unfortunately, coherent processing systems are also contaminated with coherent artifact noise, which is regarded as the number one enemy of coherent processings. In addition, coherent sources are expensive and the processing environment is usually critical.

Many optical information processing operations can be implemented by systems that use extended polychromatic light sources; however, the schemes are not without pitfalls. The partially coherent processing system is capable of reducing the inevitable artifact noise, but generally introduces a dc-bias build-up problem, resulting in poor processing performance.

We have shown that image subtraction can be achieved by the use of an extended incoherent source[3,4]. The question to be addressed is, to what degree can we relax the coherence requirements without sacrificing the processing capabilities of the processing system. The nature of each optical processing operation governs the temporal and spatial coherence requirements necessary to obtain satisfactory results. We will reduce the general formulas we have obtained, in the previous section, to suit the image subtraction application under consideration. In the following we will discuss the temporal and spatial coherence requirements for the image subtraction operation.

3.2 Coherence Requirement for Image Subtraction

In a recent paper published by Wu and Yu [3], a technique of image subtraction with an encoded incoherent source is described. Fig. 3-1 illustrates the processing system for image subtraction. An extended incoherent source with an encoding mask is placed at plane P_0; the two object transparencies to be subtracted are located at plane P_1. A sinusoidal grating (either a phase or amplitude grating) in Fourier plane P_2 acts as a spatial filter to perform the subtraction operation. With the reduced spatial coherence, image subtraction can also be obtained with a source encoding mask. In this section the coherence requirments, which depend on the source size and the spectral bandwidth of the light source, will be evaluated for the image subtraction.

3.2.1 Basic Formulas

The approch will consist of calculating the propagation of the mutual intensity function through the optical processor that utilizes an encoded source of extended size. With reference to the partially coherent optical processing system of Fig. 3-1, the encoded source intensity distribution can be written
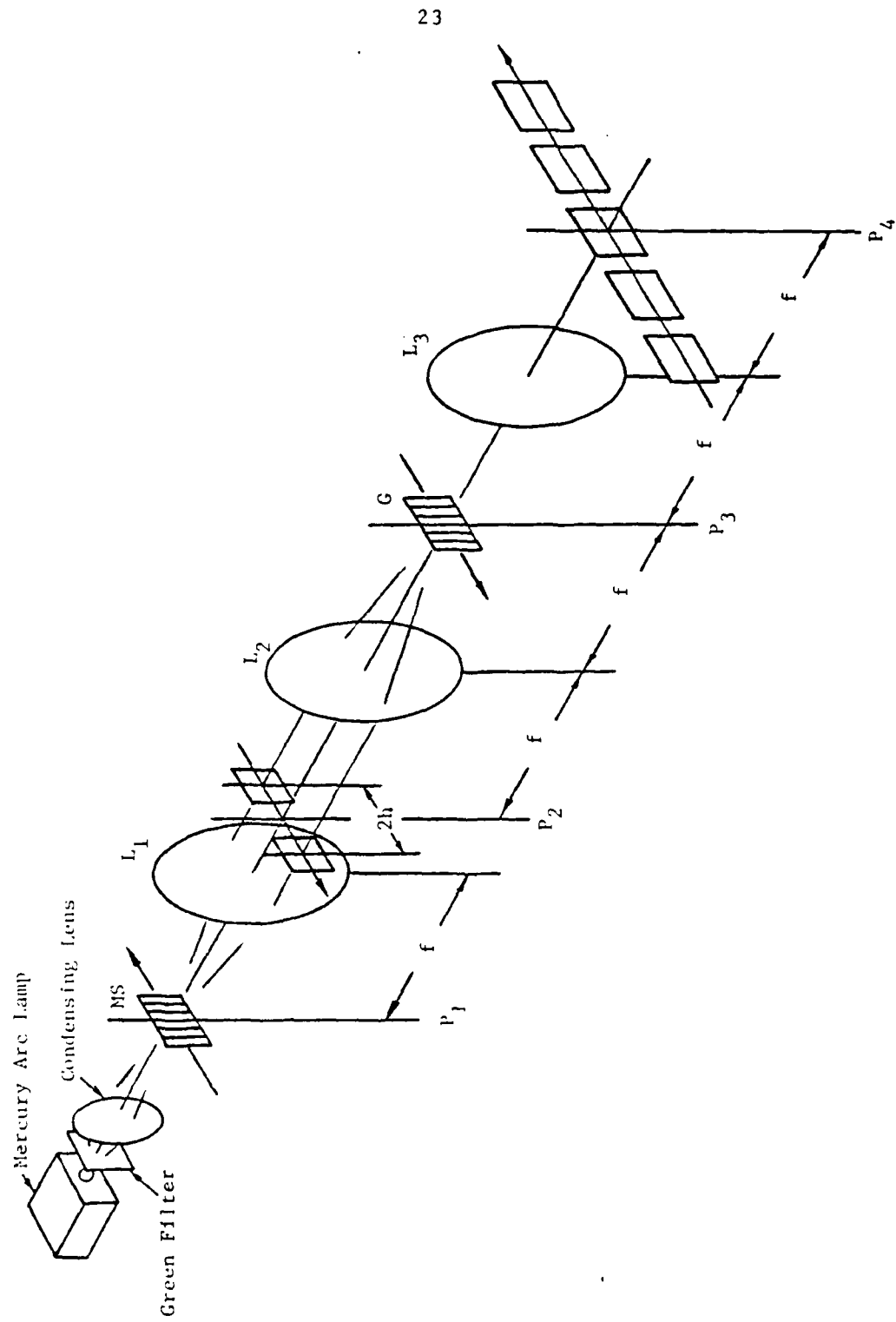
Figure 3-1. Partially Coherent Optical Processing System for Image Subtraction.

$$\gamma(x_o y_o) = \text{rect}(\frac{x_o}{d'}) * \sum_{n=-N}^{N} \delta(x_o - nD') \quad , \qquad (3-1)$$

where * denotes the convolution operation, D' is the spacing of the encoding slits, d' is the slit width and $2N+1$ is the total number of encoding slits, as depicted in Fig. 3-2. Since the image subtraction is a one-dimensional processing operation, a one-dimensional notation will be adopted for the discussion. Thus, from Eq.(2-22), the encoded mutual intensity function at the input plane can be written as

$$J(x_1 - x_2; \lambda) = \int_{-\infty}^{\infty} \text{rect}(\frac{x_o}{d'}) * \sum_{n=-N}^{N} \delta(x_o - nD') \exp[-j\frac{2\pi}{\lambda f}(x_1 - x_2)x_o] dx_o$$

$$= \int_{-\infty}^{\infty} \text{rect}(\frac{x_o}{d'}) \exp[-j\frac{2\pi}{\lambda f}(x_1 - x_2)x_o] dx_o$$

$$\times \int_{-\infty}^{\infty} \sum_{n=-N}^{N} \delta(x_o - nD') \exp[-j\frac{2\pi}{\lambda f}(x_1 - x_2)x_o] dx_o$$

$$= \sum_{n=-N}^{N} \text{sinc} \frac{d'(x_1 - x_2)}{\lambda f} \exp[-j\frac{2\pi}{\lambda f}(x_1 - x_2)nD'] \quad . \qquad (3-2)$$

The two object transparencies, in Fig. 3-1, $A(x)$ and $B(x)$ are placed at the input plane P_1. They can be expressed as .
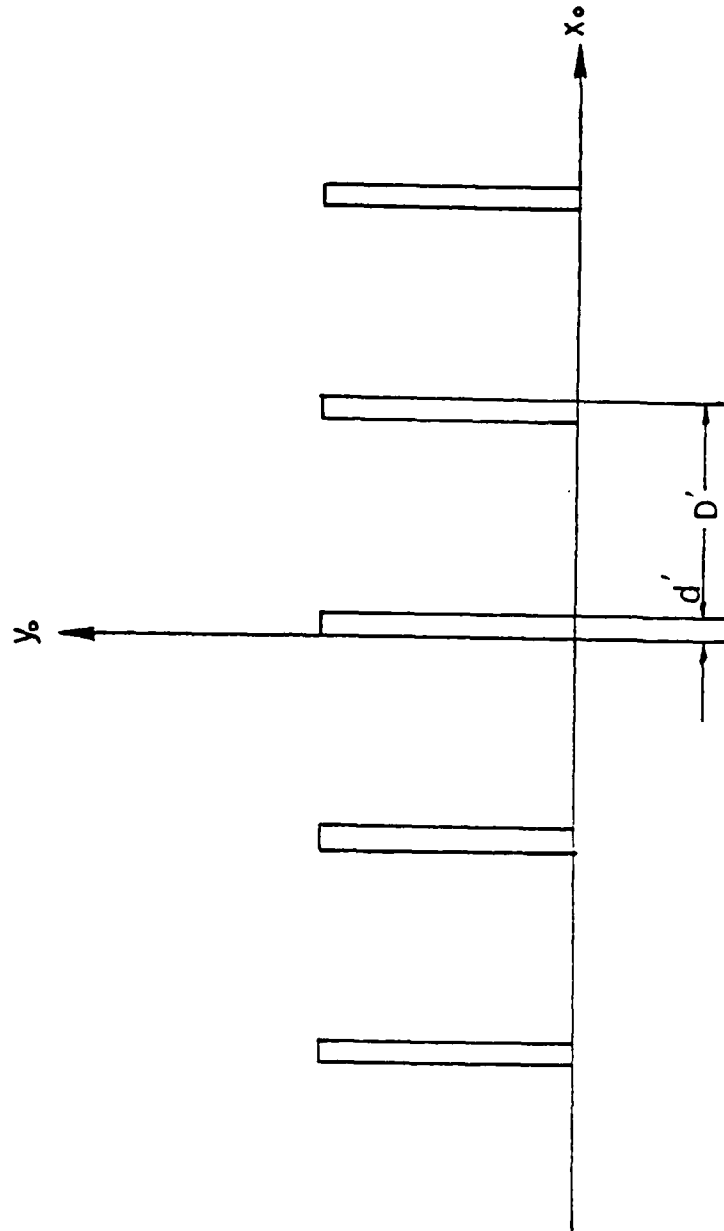
Figure 3-2. Source Encoding Mask.

$$s(x)=A(x-h)+B(x+h) \quad , \tag{3-3}$$

where 2h is the separation between the transparencies. From Eq. (3-2) the mutual intensity function at the spatial frequency plane P_2, is

$$J(x_1,\alpha_2;\lambda)=\sum_{n=-N}^{N}\int\int_{\infty}^{\infty} \text{sinc}[\frac{d'(x_1-x_2)}{\lambda f}]\exp[-j\frac{2\pi}{\lambda f}(x_1-x_2)nD']$$

$$x \ [A(x_1-h)+B(x_1+h)][A^*(x_2-h)+B^*(x_2+h)]$$

$$x \ \exp[-j\frac{2\pi}{\lambda f}(\alpha_1 x_1-\alpha_2 x_2)]dx_1 dx_2 \quad . \tag{3-4}$$

In the image subtraction operation, a sinusoidal grating with spatial frequency ν_o is placed at the Fourier plane. The mutual intensity function immediately behind the grating is

$$J'(\alpha_1,\alpha_2;\lambda)=J(\alpha_1,\alpha_2;\lambda)(1+c\sin 2\pi\nu_o\alpha_1)(1+c\sin 2\pi\nu_o\alpha_2) \quad . \tag{3-5}$$

The intensity distribution at the output plane P_3, for a given λ is therefore

$$I(x';\lambda)=\int\int J'(\alpha_1,\alpha_2;\lambda)\exp[-j\frac{2\pi}{\lambda f}(\alpha_1-\alpha_2)x']d\alpha_1 d\alpha_2 \quad . \tag{3-6}$$

By using Eqs. (3-4) and (3-5), Eq. (3-6) becomes

$$I(x';\lambda)=\sum_{n=-N}^{N}\iint sinc[\frac{d'(x_1-x_2)}{\lambda f}]exp[j\frac{2\pi}{\lambda f}(x_1-x_2)nD']$$

$$x\ [A(x_1-h)+B(x_1+h)][A^*(x_2-h)+B^*(x_2+h)]$$

$$x\ \iint(1+csin2\pi\nu_o\alpha_1)(1+csin2\pi\nu_o\alpha_2)exp[-j\frac{2\pi}{\lambda f}(\alpha_1x_1-\alpha_2x_2)]$$

$$x\ exp[-j\frac{2\pi}{\lambda f}(\alpha_1-\alpha_2)x']d\alpha_1d\alpha_2\}dx_1dx_2 \qquad . \tag{3-7}$$

It is easy to show that the second integral in Eq. $(3-7)$ is equal to

$$\int_{-\infty}^{\infty}\int(1+csin2\pi\nu_o\alpha_1)(1+csin2\pi\nu_o\alpha_2)exp[-j\frac{2\pi}{\lambda f}(\alpha_1x_1-\alpha_2x_2)]$$

$$x\ exp[-j\frac{2\pi}{\lambda f}(\alpha_1-\alpha_2)x']d\alpha_1d\alpha_2$$

$$=[\delta(x_1-x')+\frac{c}{2j}\delta(x_1-x'-\lambda f\nu_o)-\frac{c}{2j}\delta(x_2-x'+\lambda f\nu_o)]$$

$$x\ [\delta(x_2-x')+\frac{c}{2j}\delta(x_2-x'-\lambda f\nu_o)-\frac{c}{2j}\delta(x_2-x'+\lambda f\nu_o)] \qquad . \tag{3-8}$$

By substituting Eq. $(3-8)$ into Eq. $(3-7)$, and after a tedious calculation $I(x';\lambda)$ can be written

$$I(x';\lambda)=N(|A(x'-h)+B(x'+h)|^2)$$

$$+ \frac{Nc^2}{4}[2\mathrm{sinc}(2\pi d\nu'_o)\mathrm{Re}\{A(x'-h+\lambda f\nu_o)B(x'+h-\lambda f\nu_o)$$

$$-|A(x'-h+\lambda f\nu_o)|^2-|B(x'+h-\lambda f\nu_o)|^2$$

$$-|A(x'-h-\lambda f\nu_o)|^2-|B(x'+h+\lambda f\nu_o)|^2 \quad , \tag{3-9}$$

where $\mathrm{Re}\{f(x)\}$ represents the real part of function $f(x)$. Eq. (3-9) illustrates that there will be six difraction terms at the output plane if we choose $\nu_o = h/\lambda f$. Considering only the diffraction terms which are around the optical axis, we have

$$I^{(0)}(x';\lambda)=|A(x'-h+\lambda f\nu_o)|^2-2\mathrm{sinc}(2\pi d\nu'_o)$$

$$x \; \mathrm{Re}\{A(x'-h+\lambda f\nu_o)B(x'+h-\lambda f\nu_o)$$

$$+|B(x'+h-\lambda f\nu_o)|^2 \quad . \tag{3-10}$$

From Eq. (3-10) it is noted that if the slit size d equals zero, the analysis reduces to the case of strict spatial coherence with the intensity distribution given by

$$I^{(0)}(x';\lambda)\Big|_{d=0} =[A(x')-B(x')]^2 \quad . \tag{3-11}$$

Eqs.(3-10) and (3-11) show that a perfect subtracted image requires a strictly spatial coherent system, and the quality of the subtracted image decreases as the slit size increases.

To analyze the case of partial coherence assume that the light source has a uniform spatial bandwidth and that the spectral response of the detector is also uniform [i.e., $S(\lambda)=k; C(\lambda)=k$]. In this case the image intensity distribution at the output plane may be given by

$$
I^{(0)}(x') = \int_{\lambda_0-\Delta\lambda/2}^{\lambda_0+\Delta\lambda/2} I(x';\lambda)d\lambda
$$

$$
= \int_{\lambda_0-\Delta\lambda/2}^{\lambda_0+\Delta\lambda/2} \left|A(x'-h+\lambda f\nu_0)\right|^2 - 2\,\mathrm{sinc}(2\pi d\nu_0)
$$

$$
\times \, \mathrm{Re}\{A(x'-h+\lambda f\nu_0)B(x'+h-\lambda f\nu_0)\}
$$

$$
+ \left|B(x'+h-\lambda f\nu_0)\right|^2 d\lambda \; . \tag{3-12}
$$

For polychromatic illumination the spatial frequency of the diffraction grating, ν_0, is chosen to be $\nu_0 = h/\lambda_0 f$, where λ_0 is the center wavelength, and $\Delta\lambda$ is the spectral bandwidth of the light source. Changing the variable λ to $\lambda' = \lambda - \lambda_0$, Eq.(3-12) becomes

30

$$I^{(0)}(x') = \int_{-\Delta\lambda/2}^{\Delta\lambda/2} \{|A(x'-\lambda'f\nu_o)|^2 - 2\text{sinc}(2\pi d\nu_o')$$

$$\times \text{Re}[A(x'+\lambda'f\nu_o)B(x'-\lambda'f\nu_o)]$$

$$+|B(x'-\lambda'f\nu_o)|^2\}d\lambda' \quad . \tag{3-13}$$

Eq. (3-13) may be simplified by using a Taylor series expansion for the input object functions, i.e.,

$$A(x'+\lambda'f\nu_o) = A(x') + \sum_{m=1}^{\infty} \frac{1}{m!} A^{(m)}(x')(\lambda'f\nu_o)^m \quad , \tag{3-14a}$$

and

$$B(x'-\lambda'f\nu_o) = B(x') + \sum_{m=1}^{\infty} \frac{(-1)^m}{m!} B^{(m)}(x')(\lambda'f\nu_o)^m \quad , \tag{3-14b}$$

where

$$A^{(m)}(x') = d^m A(x')/dx'^m \quad . \tag{3-15a}$$

and

$$B^{(m)}(x') = d^m B(x')/dx'^m \quad . \tag{3-15b}$$

Therefore we find that

$$I^{(0)}(x') = \{|A(x')|^2 + 2\text{sinc}(2\pi d\nu_o')A(x')B(x') + |B(x')|^2 \}\Delta\lambda$$

$$+ \sum_{\substack{m=\text{even} \\ m=0}} \frac{1}{2^{m+1}(m+1)!}(f\nu_o)^m [A^{(m)}(x')-\text{sinc}(2\pi d\nu_o')N^{(m)}(x')]$$

$$x\ [A(x')+B(x')](\Delta\lambda)^{m+1}$$

$$+ \sum_{\substack{m \\ m+m'=\text{even} \\ m=0 \\ m'=0}} \sum_{m'} \frac{1}{2^{(m+m'-1)}(m+m'+1)m!m'!}(f\nu_o)^{m+m'}\{A^{(m)}(x')A^{(m')}(x')$$

$$-(-1)^{m'}\text{sinc}(2\pi d\nu_o')A^{(m)}(x')B^{(m')}(x')$$

$$+(-1)^{m+m'}B^{(m')}(x')\}(\Delta\lambda)^{m+m'+1} \quad . \qquad (3-16)$$

This equation shows that a high contrast subtracted image can be obtained with object transparencies of moderately low spatial frequency content. In addition this equation may be used to compute the spectral requirement of the light source.

An example analysis will now be presented to develop the modulation transfer function (MTF). These will be used to determine the temporal and spatial coherence requirements of the image subtraction process. Assume that the input object transparencies are

$$A(x)=1 \quad , \qquad (3-17a)$$

and

$$B(x)= \frac{1}{2}\ [1+C_o\cos(2\pi_o x)] \quad , \qquad (3-17b)$$

where ν is the spatial frequency of the test object. Then the intensity of the subtracted image is

$$I^{(0)}(x') = \int_{-\Delta\lambda/2}^{\Delta\lambda/2} \{1 - 2\text{sinc}(2\pi d\nu_o')[\frac{1}{2} + \frac{C_o}{2}\cos 2\pi\nu(x'-\lambda' f\nu_o)]$$

$$+[\frac{1}{2} + \frac{C_o}{2}\cos 2\pi\nu(x'-\lambda' f\nu_o)]^2\} d\lambda'$$

$$=[\frac{3}{4} - \frac{C_o^2}{8} - \text{sinc}(2\pi d\nu_o')]\Delta\lambda + C_o[\frac{1}{2} - \text{sinc}(2\pi d\nu_o')]$$

$$x \ \text{sinc}(\pi f\nu_o\Delta\lambda)\Delta\lambda\cos(2\pi\nu x')$$

$$+ \frac{C_o}{8} \text{sinc}(2\pi f\nu_o\Delta\lambda)\Delta\lambda\cos 2\pi(2\nu)x' \quad . \tag{3-18}$$

For this equation it is evident that in addition to the basic frequency term $[\cos(2\pi\nu x')]$, there is a second harmonic term $[\cos 2\pi(2\nu)x']$ that appears at the output plane. The corresponding contrast measures can be, respectively, written as

$$\gamma_p(\nu) = \frac{2C_o[1 - 2\text{sinc}(2d\nu_o')]\text{sinc}(\nu\nu_o\Delta\lambda)}{\frac{3}{4} - \frac{C_o^2}{8} - \text{sinc}(2d\nu_o')} \quad , \tag{3-19a}$$

and

$$\gamma_p(2\nu) = \frac{\frac{C_o^2}{8} \sin(2f\nu\nu_o\Delta\lambda)}{\frac{5}{4} - \frac{C_o^2}{8} \operatorname{sinc}(2d\nu_o')} \quad . \tag{3-19b}$$

From these equations, it can be seen that the subtracted image depends on the spatial frequency of the input object, ν, and the spectral bandwidth of the light source $\Delta\lambda$. Thus, a high spatial frequency input object and a broad spectral band of light source will result in a lower contrast of the subtracted image. In contrast, if $\Delta\lambda = 0$ and $d' = 0$ (i.e., a coherence case), the subtracted image produces a contrast reversed image. The corresponding intensity distribution is

$$\bar{I}_o(x') = [A(x') - B(x')]^2$$

$$= [1 - \frac{1}{2} - \frac{C_o}{2} \cos(2\pi\nu x')]^2 \quad .$$

$$= \frac{1}{4} - \frac{C_o^2}{8} - \frac{C_o}{2} \cos(2\pi\nu x') - \frac{C_o'}{8} \cos 2\pi(2\nu)x' \quad . \tag{3-20}$$

Thus, the corresponding contrasts of the basic and second harmonic frequencies are

$$\gamma_c(\nu) = 4C_o/(2 - C_o^2) \quad , \tag{3-21a}$$

and

$$\gamma_c(\nu) = C_o/(2 - C_o^2) \quad , \tag{3-21b}$$

respectively.

The MTF is defined as the ratio of the contrast of

Table 3-3. The Spatial Coherence Requirement for Different d'/D'

d'/D'	0.05	0.1	0.2	0.3
MTF	0.85	0.57	0.18	0.006
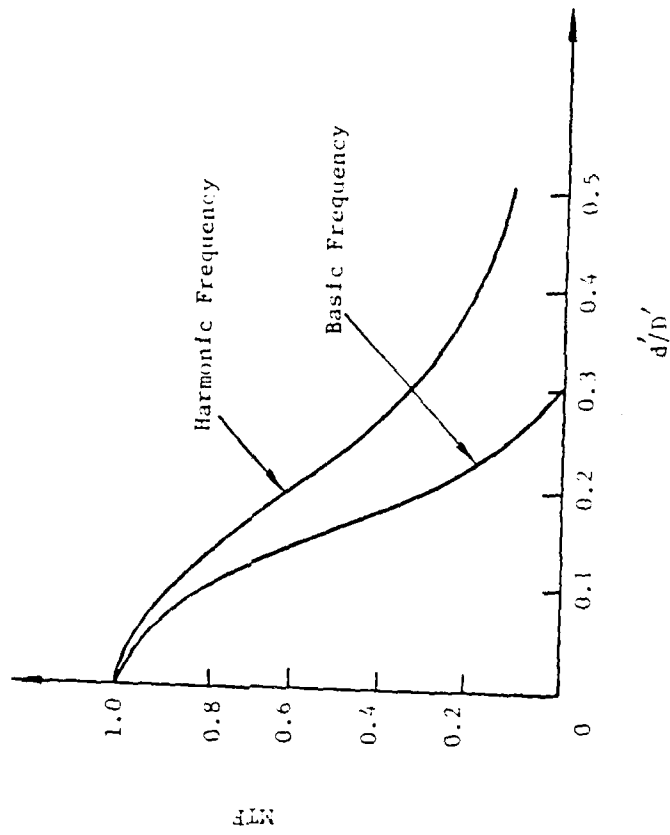
Figure 3-8. Apparent Modulation Transfer Function vs. the Ratio of the Slit Width to Spatial Period d'/D'.

mask (i.e., d'/D'). To obtain a high degree of spatial coherence for a subtraction operation, a lower ratio of d/D should be maintained. The dependence of the modulation transfer function on d'/D' is plotted in Fig. 3-8. From this figure it can be seen that when $d'/D'=0.3$, the MTF approches zero, and the subtraction operation ceases to function. If the ratio of d'/D' is sufficiently small, a higher MTF can be obtained. A few numerical examples are provided in Table 3-3.

From this table it is clear that for $d'/D'=0.05$, a relatively high MTF=0.85 can be obtained for the subtraction operation. To obtain a higher contrast of the subtracted image a smaller ratio of d'/D' is required.
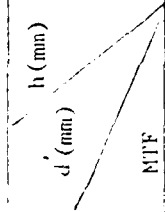
In addition, the MTF decreases rather rapidly as the ratio of the slit width, d', to the focal length of the transform lens, f, (i.e., d'/f) increases. Thus, if the focal lengths of the collimating and transfer lenses are set equal to one unit of the horizontal axis, Fig. 3-7 will represent the slit width of the encoding mask.

Since the visibility of the subtracted image depends on the modulation transfer function, with required MTF and h, the appropriate source size can be determined. The effects between the MTF, the separation h, and the source size are tabulated in Table 3-2, where the focal length of the Fourier transform lens was assumed to be 300 mm

Table 3-2 shows that a very narrow source size, d', is required for a high modulated transfer function. However, such a small incoherent source is difficult to achieve in practice. This difficulty can be alleviated with a source encoding technique. The discussion of this technique follows.

A multislit source encoding mask is used for illustration. Note that the spatial period of the encoding mask should be precisely equal to that of the diffraction grating, G (i.e., $d=1/\nu_o$). In other words, the modulation transfer function of Eqs. (3-25) and (3-26) has sinc(2 d'/D'). That is, the spatial coherence requirement is independent of the slit size, but it depends on the ratio of slit width to the spatial period of the encoding

Table 3-2 The Source Size for Image Subtraction under

Different MTF and Separation h. f=300 mm.

d'(mm) / MTF \ h (mn)	5.0	7.5	10.0
0.1	0.0076	0.005	0.0038
0.3	0.0052	0.0035	0.0026
0.6	0.0031	0.0021	0.0015
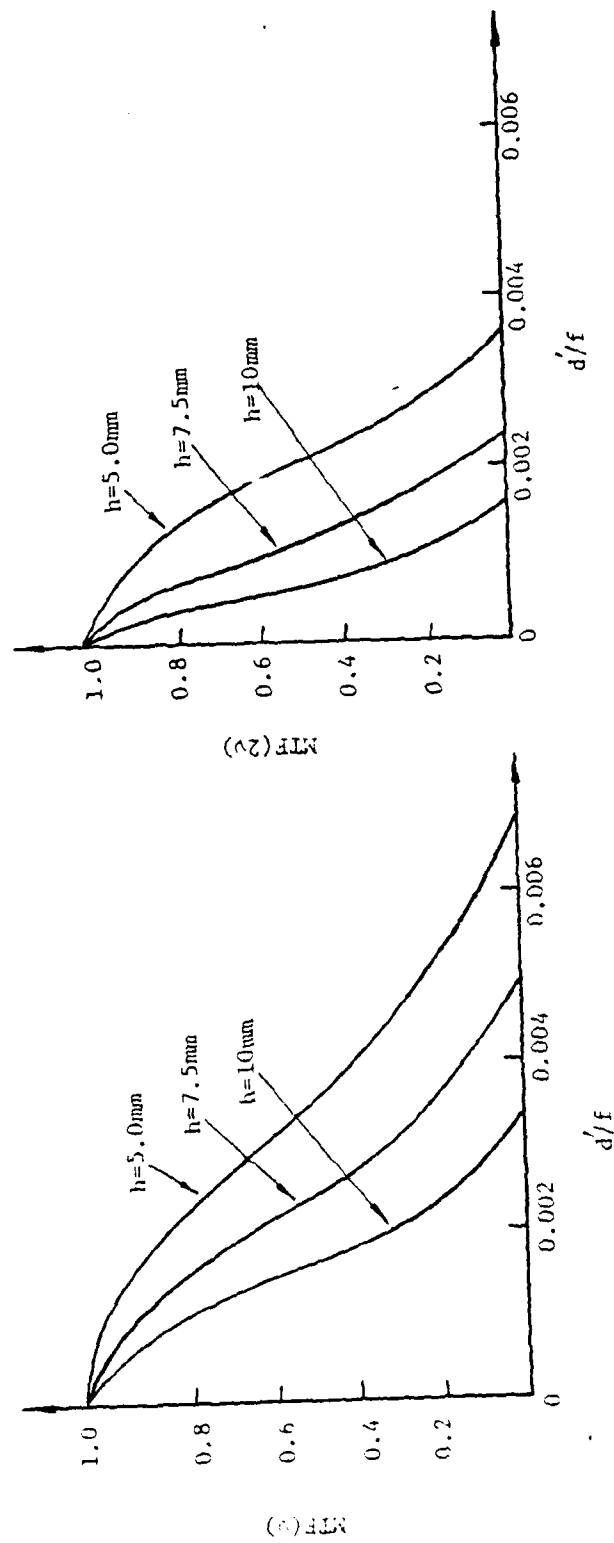
Figure 3-7. MTF(ν) and MTF($2-\nu$) vs. d'/f for Various Separation h, d' is Slit Width and f is the Focal Length of the Transform Lens.
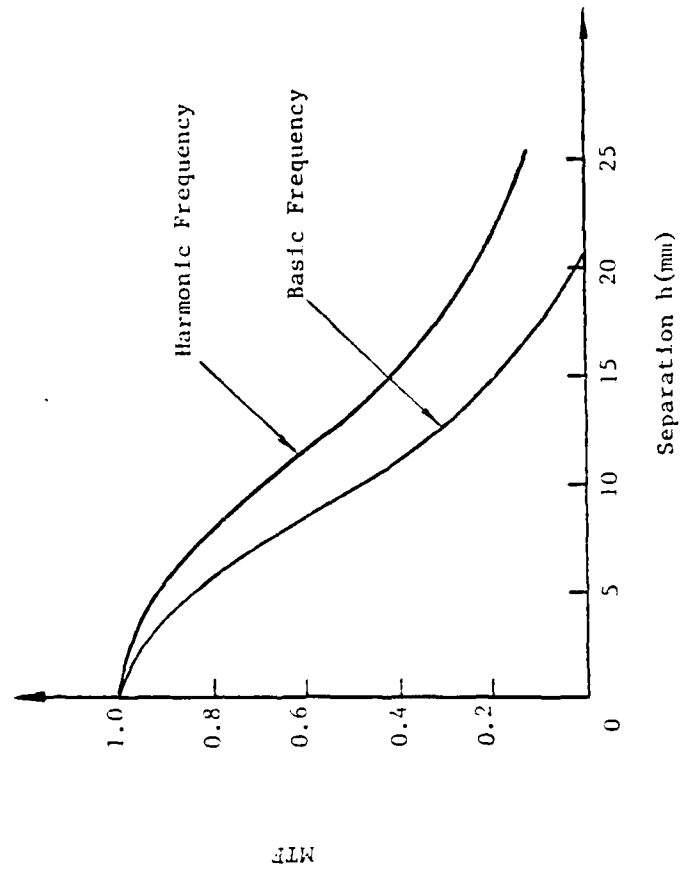
Figure 3-6. Apparent Modulation Transfer Function vs. the Separation h.

3.2.3 Spatial Coherence Requirement

Consider the case of perfect temporal coherence ($i.e.$, $\Delta\lambda=0$) and spatially partial coherence, where Eqs.(3-6 8a) and (3-68b) are of the form

$$MTF_1 = \frac{(2-C_o^2)[1-2sinc(2d\nu_o')]}{10-C_o^2-8sinc(2d\nu_o')} \quad .$$ (3-25)

$$MTF_2 = \frac{2-C_o^2}{10-C_o^2-8sinc(2d\nu_o')} \quad .$$ (3-26)
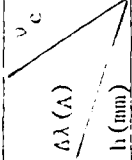
Note that the modulation transfer functions are independent of the spatial frequency of the input object.

The above equations, however, depend on the slit width d'. This requires that the grating be precisely designed to match the separation of the object transparencies, i.e.

$$\nu_o=h/\lambda_o f \quad .$$ (3-27)

The plots of the MTF versus the separation h, for Eqs.(3-25) and (3-26) are shown in Fig.3-6. It is clear that the MTF is a monotonic function of h. To obtain a high contrast subtracted image, the separation h must be reduced. However, decreasing the separation between the object transparencies limits the size of input objects to be processed.

Table 3-1   Temporal Coherence Requirement for Different ν_c and h

$\Delta\lambda(\text{Å})$ / h (mm)	4	8	12	16	20
5.0	240	135	92	67	52
7.5	176	92	62	45	32
10.0	130	70	45	32	17

38

Figure 3-5. Relationship Between the Cutoff Frequency and the Spectral Bandwidth of the Light Source $\Delta\lambda$ for Various Values of Separation h. 2h is the Main Separation Between the Input Transparencies.

Figure 3-4. Relationship Between the Cutoff Frequency ν_c and the Spectral Bandwidth of the Light Source $\Delta\lambda$ for Different Minimum Desirable Contrasts C_m.
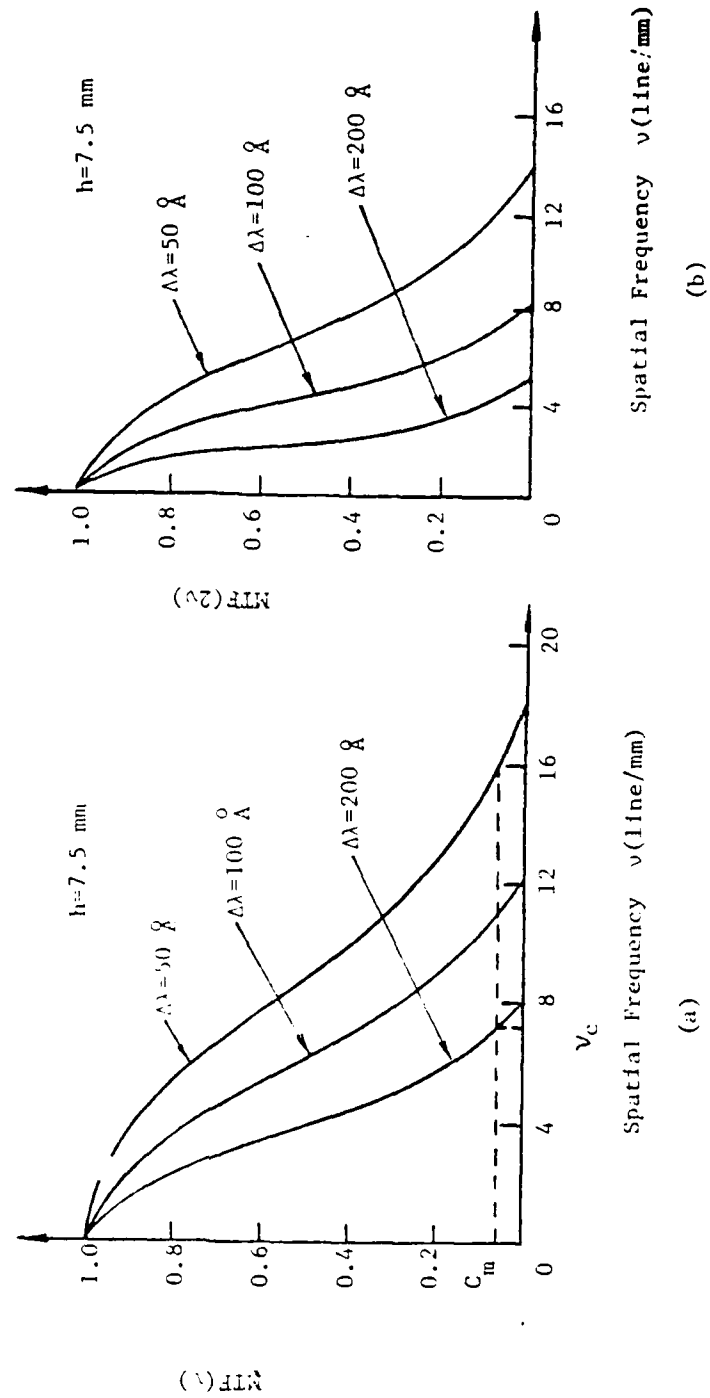
Figure 3-3. Apparent Modulation Transfer Function for a
Partially Coherent Image Subtraction:
(a) Basic Frequency;
(b) Second Harmonic.

The normalized MTF curves of the basic and harmonic
freq·encies are shown in Fig. 3-3. It is obvious that the
contrast of the subtracted image decreases monotonically
as a function of the object spatial frequency. However,
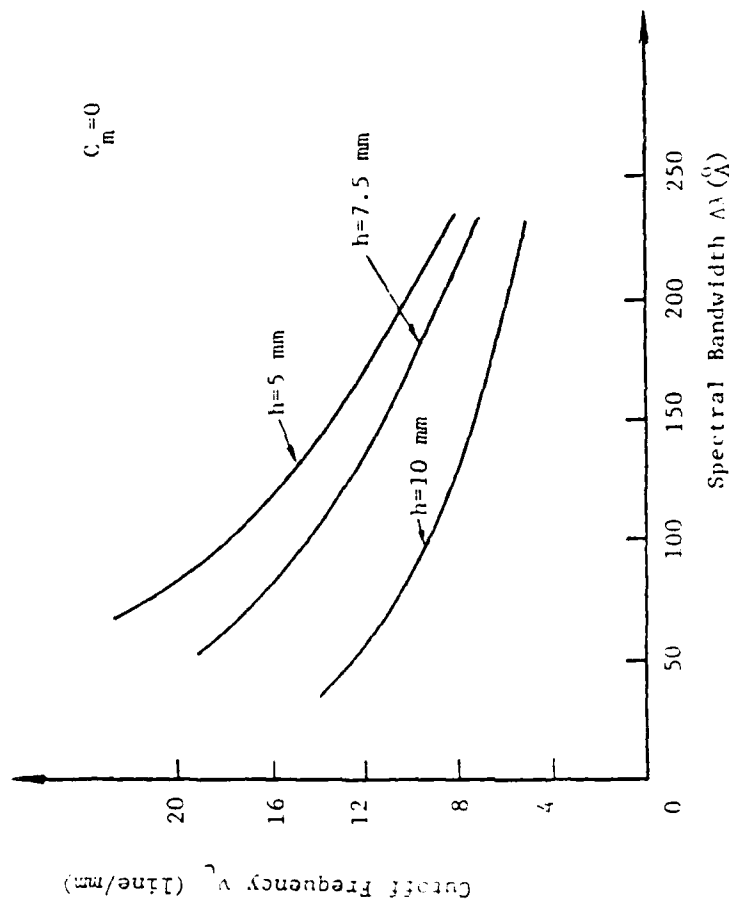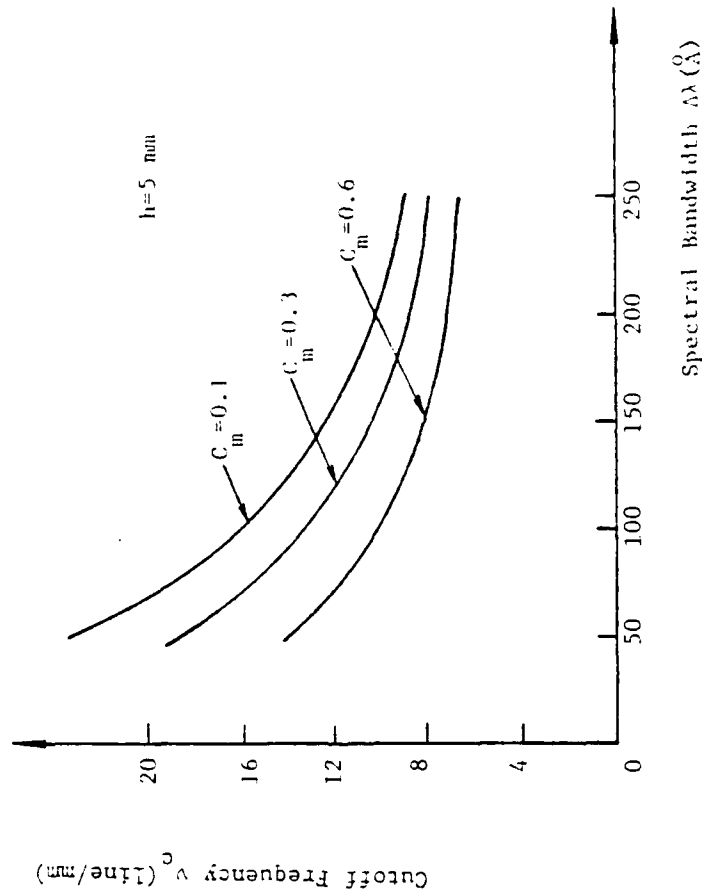the MTF of the subtracted image decreases as the spectral
bandwidth of the light source increases. In other words,
the quality of the subtracted image improves as the
spectral bandwidth of the light source and the spatial
frequency of the object decrease. We define ν_c to be the
cut-off spatial frequency when the MTF decreases to a
minimum value C_m, as shown in Fig. 3-3. The value C_m
depends on the maximum resolution of the output recording
material. Fig. 3-4 shows tne functional relationship of
the cut-off frequency ν_c and the spectral width $\Delta\lambda$ for
various values of C_m. It is possible to determine the
spectral bandwidth requirement from this figure. The
relationship between the cut-off frequency ν_c , the
spectral width $\Delta\lambda$ and the separation between the two input
transparencies h is shown in Fig. 3-5. Note that the
spectral bandwidth required, for a given cut-off
frequency, decreases with increasing separation h.
Table 3-1 illustrates the dependence of $\Delta\lambda$ on ν_c and h.
The focal length of the Fourier transform lens was
selected as f=300 mm for the calculations. It is clear
from the table that, as the spatial frequency and object
separation increase, the spectral bandwidth of the light
source must decrease.

the input and output sinusoidal objects. From Eq. (3-19) and (3-21) these are given by

$$MTF(\nu) = \frac{[1-2\mathrm{sinc}(2d\nu_0')](2-dC_0'^2)\mathrm{sinc}(f\nu\nu_0\Delta\lambda)}{10-C_0^2-8\mathrm{sinc}(2d\nu_0')} \quad , \qquad (3\text{-}22a)$$

$$MTF(2\nu) = \frac{(2-C_0^2)\mathrm{sinc}(2f\nu\nu_0\Delta\lambda)}{10-C_0^2-8\mathrm{sinc}(2d\nu_0')} \quad . \qquad (3\text{-}22b)$$

As previously stated, Eqs.(3-68a) and (3-68b) will allow the evaluation of the temporal and spatial coherence requirements for image subtraction.

3.2.2 The Temporal Coherence requirement

The case of strictly spatial coherence will be discussed first. This requires that the slit size d of the encoding mask approach zero. Eqs.(3-22a) and (3-22b) are then reduced to

$$MTF(\nu) = \mathrm{sinc}(f\nu\nu_0\Delta\lambda) \quad , \qquad (3\text{-}23)$$

$$MTF(2\nu) = \mathrm{sinc}(2f\nu\nu_0\Delta\lambda) \quad . \qquad (3\text{-}24)$$

IV. Resolution Limit

It is known that the resolution limit is affected by the coherence requirement and the space bandwidth product of the processing system. We shall now discuss in detail these two factors.

4.1 Effect Due to Coherence Requirement

We shall first discuss the effect on resolution limit due to temporal coherence requirement. We note that for the case of strict spatial coherence, the slit width d of the source encoding mask should approach zero. Thus the MTF of Eqs. (3-22a) and (3-22b) becomes,

$$MTF(\omega) = sinc(ph \frac{\Delta\lambda}{\lambda_o}), \tag{4-1}$$

$$MTF(2\omega) = sinc(2ph \frac{\Delta\lambda}{\lambda_o}), \tag{4-2}$$

where d = 0, the normalized MTF curves of the fundamental and second harmonic frequencies are shown in Figure 3-3. It is obvious that the contrast of the subtracted image decreases monotonically as a function of the input object spatial frequency, for a given separation. The MTF of the subtracted image also decreases as the spectral bandwidth of the light source. In other words, the quality of the subtracted image improves for narrower spectral bandwidth of the light source and lower spatial frequency of the object.

Let us define p_c be the resolution limit of the subtracted image, where the MTF decreases to a minimum value C_m, as shown in Figure 3-3. Figure 3-4 shows the functional relationship of the resolution limit p_c and the spectral

Table 4-1. Effect of Resolution upon $\Delta\lambda$ and h, λ_o = 5461Å

$\Delta\lambda(\text{Å})$ ρ_c(lines/mm) h(mm)	50	25	10	5
6.0	14	30	68	137
4.0	20	41	102	205
2.0	41	82	205	410

width $\Delta\lambda$ for various values of C_m. We shall now determine the spectral bandwidth requirement $\Delta\lambda$ from this figure. The relationship between the resolution limit p_c, the spectral width $\Delta\lambda$ and the separation of the input object transparencies is depicted in Figure 3-5. We see that the resolution limit decreases monotonically as the spectral bandwidth and the separation of input objects increase. In order to have a feeling of magnitude, Table 4-1 illustrates the relation of p_c, h and $\Delta\lambda$, where the center wavelength λ_o of the light source is assumed to be 5461Å and the MTF(ω) = 0.3. Thus, we see that, to obtain a high resolution of the subtracted image, a narrow spectral band of light source is required. We shall now consider the spatial coherence requirement. The MTF of Eqs (3-22a) and (3-22b) are;

$$MTF_1 = \frac{(2 - C_o^2)[1 - 2\ \text{sinc}(2dp_o)]}{10 - C_o^2 - 8\ \text{sinc}(2dp_o)} \quad , \tag{4-3}$$

and

$$MTF_2 = \frac{2 - C_o^2}{10 - C_o^2 - 8\ \text{sinc}(2dp_o)} \quad , \tag{4-4}$$

where $\Delta\lambda = 0$, $p_o = h/(\lambda_o f)$. From these equations, we see that the MTF's are independent of the object's spatial bandwidth, however, they are functions of the slit width d. The corresponding MTF versus the separation h, are plotted in Figure 3-6. Thus to obtain a high contrast subtraction image, the separation h should be small. But decreasing the separation also limits the size of input objects to be observed. The relationship between the MTF, the object separation, and the slit width is tabulated in Table 4-2, where the focal length of the Fourier transform lens is assumed to be 300 mm.

Table 4-2. Source Size Requirement, λ_o = 5461 Å

MTF d(mm) / H(mm)	5.0	7.5	10.0
0.1	0.0076	0.005	0.0038
0.3	0.0052	0.0035	0.0026
0.6	0.0031	0.0021	0.0015

d/D	.05	.10	.20	.30
MTF	.85	.57	.18	.006

Table 4-3. Spatial Coherence Requirement for Various d/D, λ_o = 5461Å.

From this table, we see that, to maintain an adequately high MTF, a very narrow source is required. However a high intensive narrow source is difficult to obtain in practice. Nevertheless, this problem can be alleviated with a source encoding technique, as illustrated in the following:

A multislit source encoding mask is used for this purpose. The spatial period of the encoding mask is precisely equal to the diffraction grating G, (i.e., $D = 1/p$). The spatial coherence requirement though independent on the slit size, is governed by the ratio of the slit width to the spatial period of the encoding mask, i.e., d/D. The ratio of d/D is adequately small to achieve a high degree of point-pair spatial coherence at the input plane. The dependence of the MTF upon d/D is shown in Figure 3-8. It is obvious that the subtraction operation ceases when the MTF approaches zero, i.e., $d/D = 0.3$. A few numerical examples are presented in Table 4-3.

V. Application to Micro-Circuit-Chip Inspection

5.1 Effect Due to Space Bandwidth Product

Since the application of image subtraction to micro-circuit-chip under inspection is a high spatial frequency type object, the transform lenses L_1 and L_2 are required to be highly diffraction limited. Here are a few commercial microscopic objectives suitable for this purpose, as tabulated in Table 5-1. The size requirement of the micro-circuit-chip under inspection (i.e., $S = h = p(4, \overline{2})$ and the resolution limit of the processing system can be calculated if a specific microscopic objective lens is selected. A few numerical examples are given

Table 5-1. Some Commercial Available Microscopic Objectives

No.	Magnification	Numerical Aperture	Field of View ϕ(mm)	Resolution Limit R(lines/mm)	Space Bandwidth Product ϕR
1	1	0.12	50	200	11000
2	1/5	0.2	15	370	5550
3	1/10	0.3	8	550	4400

in Table 5-2. For instance, if the spectral bandwidth of the incoherent source is 10Å, the slit size of the source encoding mas. is 3 μm and the No. 1 micro-scopic objective lens is used, then the optical processor has the capability of observing a micro-circuit chip width as large as 9 mm with a spatial resolution as high as 220 lines/mm. The capability is, of course, dependent upon the minimum detectable value of MTF, which is less than 7% in the above example.

5.2 Experimental Demonstration

In experimental demonstration, we insert a standard simulated micro-circuit chip transparency in one of the input apertures of the processor, as shown in Figure 5-1a, and a defective or faulty one in the other aperture, as shown in Figure 5-1b. By the comparison of these two Figures, we see that there are several links missing in Figure 5-1b. Figure 5-1c shows the subtracted image obtained at the output plane of the proposed processor. Since we have utilized an incoherent source, the coherent artifact noise in the subtracted image is substantially suppressed.

Another interesting experimental demonstration for inspection of IC mask[18] utilizing a simple white-light processor is also shown in Figure 5-2. Since the white-light source contains all the visible wavelengths, it is possible to identify the defects or faulty cracks through color spatial filtering. To demonstrate the defect detection, we assume that the Fourier spectra distribution of the IC mask is known a priori. We note that the scale of the signal spectrum is proportioned to the wavelength of the light source, a red and green color

Table 5-2. Image Subtraction Processing Capability
Δλ = 10Å, d = 0.003 mm.

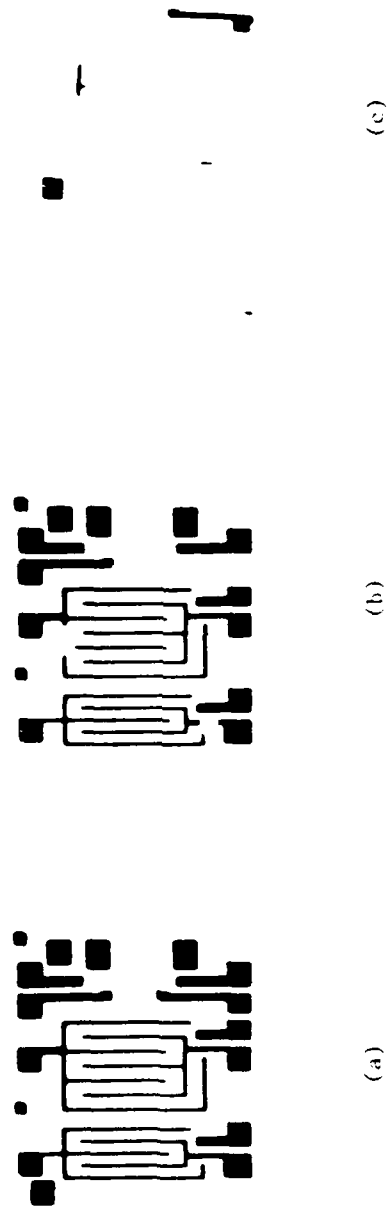| No.	S(mm)	R(lines/mm)
1	9	220
2	2.7	370
3	1.4	550

Figure 5-1.　IC Chip Inspection.　(a) and (b) are Input
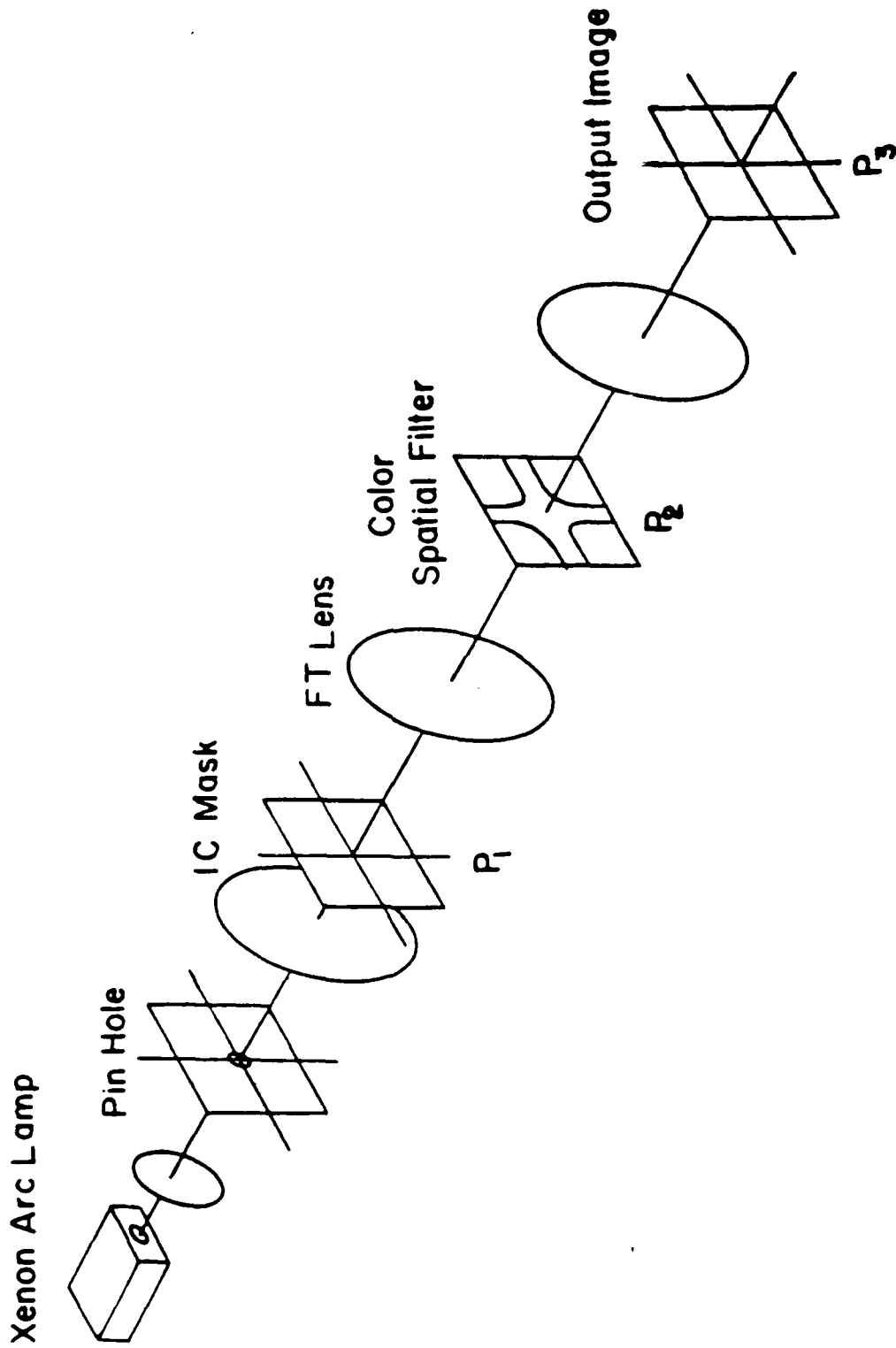Objects.　(c) Subtracted Image.

Figure 5-2. A White-light Optical Processor for IC Mask Inspection.

spatial filter, as shown in Figure 5-3a is utilized in our experiment. Since the faulty cracks are generally high spatial frequency signals, they would be expected to be diffracted outside the red color region of Figure 5-3a. Thus the faulty cracks would form green color images superimposing with red color IC mask, as shown in Figure 5-3b. From this figure, we see that the faulty cracks can be easily identified through the color coded image.

In concluding this section, we would like to point out that, it is feasible to utilize an incoherent and white-light optical processing technqiue for micro-circuit inspection. The techniques are capable of improving the reliability, efficiency and cost for large scale automatic precision inspection. They are particularly suitable for micro-circuit board inspection and robotic assembly.

VI. <u>Color Hologram Generation</u>

6.1 <u>Introduction</u>

A number of methods have been investigated for storing color images holographically on black-and-white film. The color image is then retrieved by either viewing the hologram at the proper angle when illuminated by white-light[19-21] or by placing it in a white-light optical processor where the appropriate color and spatial filtering are performed[22-23]. Because the light needed to form the hologram is coherent, the hologram and thus the reconstructed image are corrupted with coherent artifact noise. If the holographic fringes were formed with a point-pair coherence between the object and
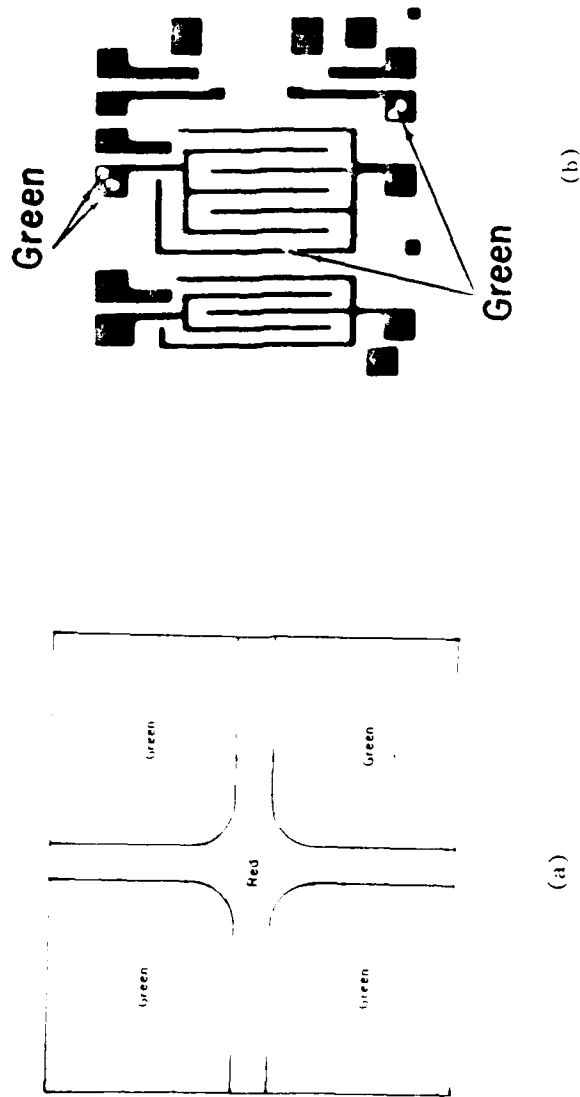
(b)

(a)

Figure 5-3.   (a)   Color Spatial Filter for IC Mask
                       Inspection.
               (b)   Color Encoded IC Mask

reference beams, derived from extended incoherent sources, the coherent noise would be suppressed. In this section, we explore the use of source encoding to establish this point-pair coherence requirement[3] and demonstrate a system that uses it to form a hologram of a 2-D color transparency. The color image is retrieved by placing the hologram in a white-light optical processor where spatial filtering is performed.

6.2 Color Hologram Construction

A system for constructing a hologra hic image of a color transparency is shown in Fig. 6-1. For simplicity, only two primary colors (i.e., red and green) are used, for the demonstration. This system is similar to the source-encoding image subtraction system as discussed in section 1.2 except the gratings are displaced at a distance ℓ from the Fourier plane P_2. At the input plane P_1, the object $0_{1(x,y)}$ is a color transparency and $0_{2(x,y)}$ is an open aperture, which acts as the reference beam. The angle at which the two beams come together at the output plane P_4 and thus the spatial frequency of the corresponding interference fringes is determined by ℓ. The frequency of each of the two gratings is chosen to be $p = kh_o/f$, where k is the wave number, h_o is the displacement of the object from the optical axis, and f is the focal length of the achromatic lens. We note that this choice of frequency will cancel the phase distribution introduced by having $0_1(x,y)$ and $0_o(x,y)$ displaced by a distance h_o from the optical axis at the input plane. Thus, we see that, as the light beams passing through the gratings, two 1st order terms will
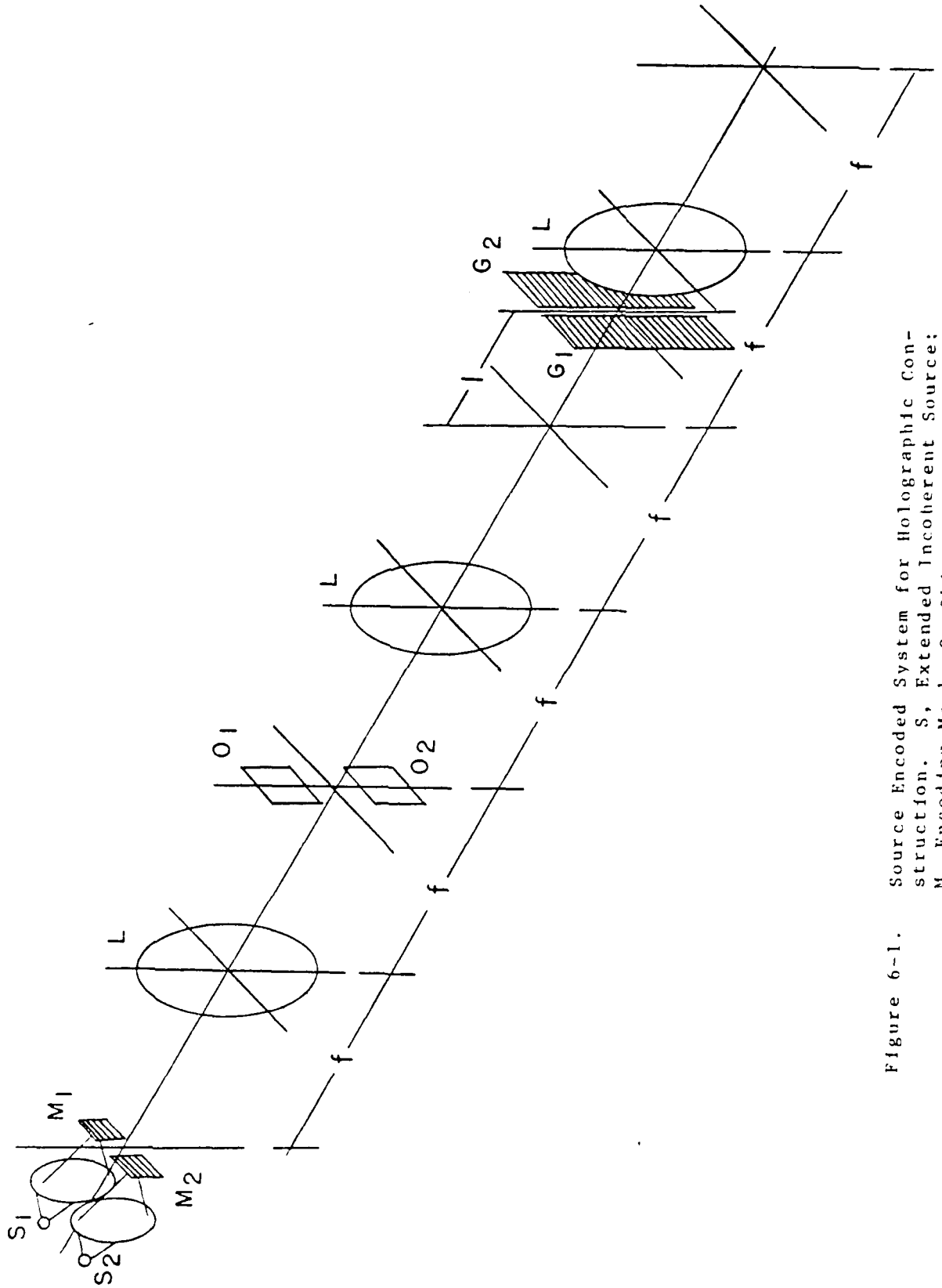
Figure 6-1. Source Encoded System for Holographic Con-
struction. S, Extended Incoherent Source;
M, Encoding Mask; O, Object; G, Phase

be bent parallel to the optical axis with the centers dis-
placed a distance of $h_1 = \pm \dfrac{h_o}{f} \ell$ respectively. These displace-
men.s introduce two phase factors of $\phi_1 = \mp \dfrac{kh_o \ell}{f^2}$ from the
object and reference beams respectively. The corresponding
complex amplitude distribution around the optical axis at
the output plane would be,

$$g(x,y) = 0_1(x,y) \ e^{-i \frac{kh\ell}{f^2} x} + 0_o(x,y) \ e^{i \frac{kh\ell}{f^2} x}. \qquad (6-1)$$

If we assumed that $0_1(x,y)$ and $0_o(x,y)$ are real functions, then
a hologram would be formed with spatial carrier frequency of
$p_o = \dfrac{2kh_o \ell}{f^2}$ in the x direction.

However, for the two beams to form interference fringes,
a mutual coherence requirement must exist between the points
of the two beams that overlap. To establish this coherence
requirement, a source encoding technique is used which estab-
lishes a coherence function at the input plane of

$$\Gamma(x) = \frac{\sin\left(N\pi \cdot \frac{xd}{\lambda f}\right)}{N \sin\left(\pi \frac{xd}{\lambda f}\right)} \ \text{sinc}\left(\pi \frac{sx}{\lambda f}\right), \qquad (6-2)$$

where s is the width of the slits of the source encoding
mask, N is the number of the encoding slits, d is the spacing
between the slits, and λ is the wavelength of the extended
light source. Thus by choosing $d = \dfrac{f\lambda}{h_o}$, we shall obtain the
proper point-pair coherence requirement for forming the holo-
graphic fringes. We shall also note that the spatial frequency
of the phase grating should be identical to the spatial
frequency of the encoding mask. Thus, separate encoding masks
and phase gratings are used for each primary color of light
sources as shown in Fig. 6-1.

Note: if the two encoding masks are separated by a distance equal to the width of the transparencies $0_1(x.y)$ and $0_0(x,y)$, the red and green light beams would be separated at plane P_3 and would be passed through each of the gratings respectively. The achromatic transform lens L_3 will then shear the two images $0_1(x\ y)$ and $0_0(x,y)$ back together, such that the red and green images will be superimposed around the optical axis at the output plane P_4 to form a spatial multiplexed color hologram.

6.3 Reconstruction of Color Image

By placing the recorded hologram in the white-light optical processor shown in Fig. 6-2, a color image would be obtained by simple spatial filtering. This process for reconstruction of the color hologram image uses the dispersion of light into different color Fourier spectra in the fourier plane. For a given spatial frequency component, the displacement of the smeared fourier spectra in the fourier plane is proportional to the wavelength of the light and the spatial frequency of the input object.

The spatial frequencies recorded on the hologram are inversely proportional to the wavelength of light which passed through that area in the original transparency when the hologram was constructed. Thus, for example: red light passing through an area of the hologram that corresponds to red on the original transparency would be diffracted to the same place in the Fourier plane of the white-light optical processor as green light passing through an area, on the hologram that corresponds to green information
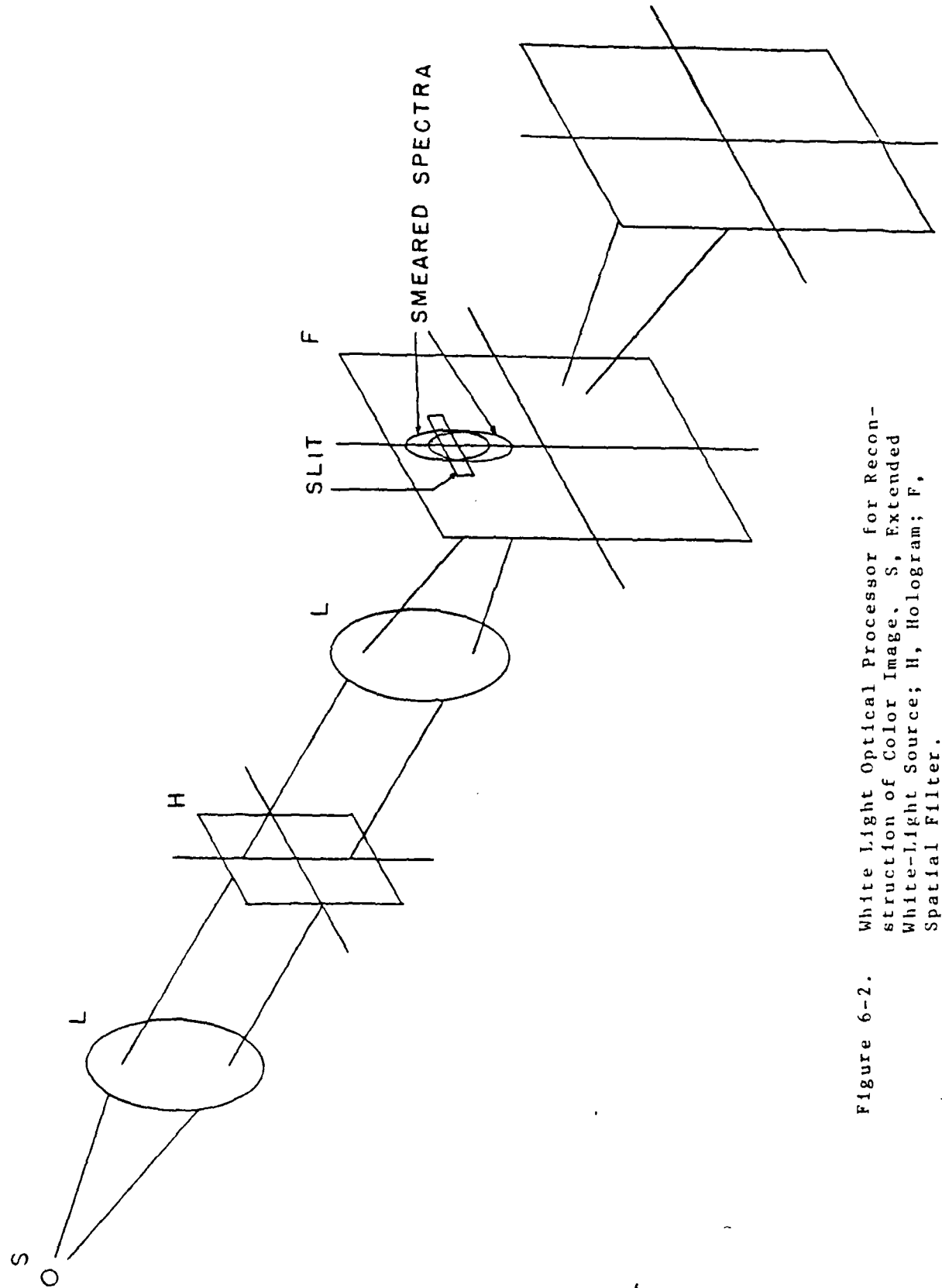
Figure 6-2. White Light Optical Processor for Recon-
struction of Color Image. S, Extended
White-Light Source; H, Hologram; F,
Spatial Filter.

on the original color transparency. By placing a narrow slit over this region of the smeared Fourier spectrum a properly colored image of the original transparency may be viewed at the output plane.

6.4 Experimental Result

In our experimental setup a mercury arc lamp with a green interference filter centered at wavelength 5460Å was used as the green source. A HeNe laser which was passed through spinning ground glass was used as the red color light source. The corresponding encoding masks have dimensions; for $s = 2.9$ μm, $d = 29$ μm, and $N = 100$, for the red encoding mask and for $s = 2.5$ μm, and $N = 100$, for the green encoding mask. The spatial period of the phase gratings were 29 μm and 25 μm for the red and green gratings respectively. The gratings were placed at approximately $\ell = f$, the focal length of the transform lens. Thus a spatial frequency of twice that of the corresponding phase grating would be encoded. For example, spatial frequencies of 34.5 ℓ/mm for the red and 40 ℓ/mm for green were recorded. Figure 3 shows the input object $O_1(x,y)$ used to construct the color hologram. Figure 6-4 is the result obtained for the reconstructed color hologram image. We note that by the noise present in the color hologram image may be reduced by placing the input objects in a liquid gate.

6.5 Remark

By using an adaptation of the source encoded image subtraction system, we were able to construct a 2-dimensional color hologram. Such a hologram offers easy white-light
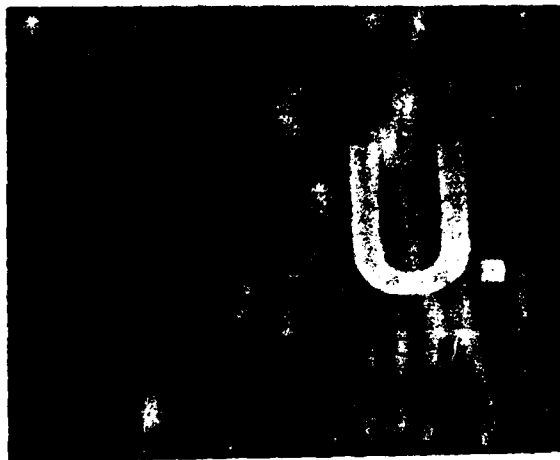
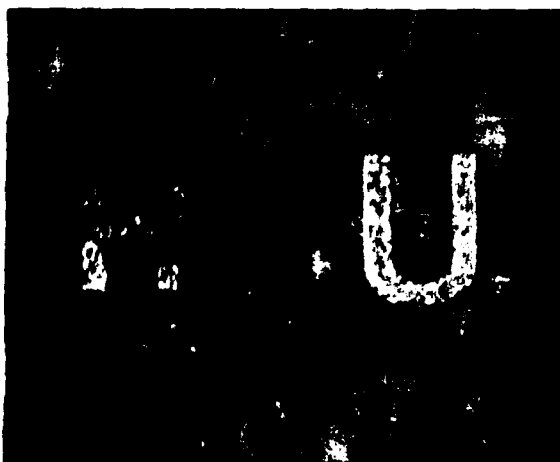Figure 6-3.   A Black-and-White Photograph of Original
Color Transparency.

Figure 6-4.   A Black-and-White photograph of Recon-
structed Color Image.

67
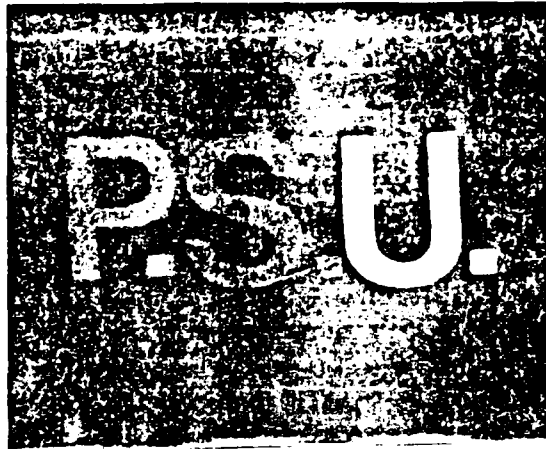

Figure 6-3.   A Black-and-White Photograph of Original
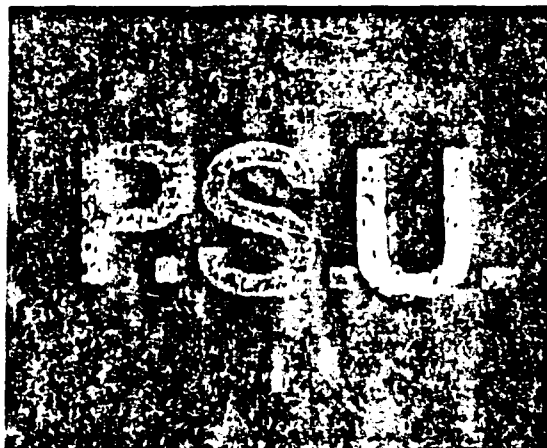   Color Transparency.

Figure 6-4.   A Black-and-White photograph of Recon-
               structed Color Image.

reconstruction of the color image and the possibility of reducing the coherent artifact noise during the construction process. Although the system was described and demonstrated with 2 primary colors it could also be extended to three colors. We would also note that the technique may also be possible to generate a 3-dimensional holographic image for phase-type object of definite depth.

VII. Conclusion

This study has led to certain definite conclusions. In particular:

1. Incoherent image subtraction processors offer a higher signal-to-noise ratio as compared with a coherent image subtraction processor.

2. The incoherent image subtraction processor is suitable for the application of tracking and identifiation for moving target.

3. It is feasible of utilizing a white-light source for image subtraction operation, a technique is currently processing.

4. The white-light image subtraction processor is capable of performing color image subtraction.

5. The image subtraction technique can also be utilized for precision industrial inspection, which would benefit the U.S. Army inspection technology and her supporting industries.

6. We have demonstrated that 2-D color holograms can be generated by image subtraction processors with extended incoherent sources.

7. The white-light image subtraction technique is
   capable of performing in a real-time mode, a
   research program is currently investigating.

The net effect of these conclusions is to emphasize
the truth of our initial assumption of the white-light image
subtraction processor can be an essential part of the
missile tracking and identification application. This
research effort in real-time tracking program should be
encouraged to pursuing.

VIII. References

1. B. D. Guenther, C. R. Christensen, and J. Upatnieks, IEEE, J. Quant. Elec., QE 15, 1348 (1979).

2. M. Born and E. Wolf, Principle of Optics, wnd rev. ed., Pergamon Press, New York, 1964.

3. S. T. Wu and F. T. S. Yu, Appl. Opt., 20, 4082 (1982).

4. F. T. S. Yu, Optical Information Processing, Wiley-Interscience, New York, 1983.

5. F. T. S. Yu and A. Tai, Appl. Opt., 18, 2705 (1979).

6. E. Verdet, Ann. Scientif, L'Ecole Normal Superienre, 2, 291 (1865).

7. A. A. Michelson, Phil. Mag. (5), 30, 1 (1890).

8. M. Berek, Z. Phys., 36, 675, 824 (1926).

9. P. H. Van Cittert, Physica, 1, 201 (1934).

10. F. Zernike, Physica, 5, 785 (1938).

11. H. H. Hopkins, Pro. Roy. Soc., A, 208, 263 (1951): ibid. A, 217, 408 (1953).

12. M. Born and E. Wolf, Principles of Optics (Pergamon. New York, 1977).

13. F. T. S. Yu, Opt. Commun., 27, 23 (1978).

14. J. W. Goodman, Introduction to Fourier Optics (McGraw-Hill, New York, NY, 1968).

15. F. T. S. Yu, Introduction to Diffraction, Information Processing and Holography (MIT Press, Cambridge, Mass., 1973).

16. F. T. S. Yu, Appl. Opt., 17, 3571 (1978).

17. F. T. S. Yu and A. Tai, Appl. Opt., 18, 2705 (1979).

18. A. Iwamoto and H. Sekizawa, Appl, Opt., 20, 1724 (1981).

19. Y. N. Denisyuk, Sov. Phys., Doklady 7, 543 (1962).

20. P. Hariharan, Wi H. Steel and Z. S. Hegedus, Opt. Lett., 1, 81 (1977).

21. H. Chen, A. Tai and F. T. S. Yu, Appl. Opt. 17, 1490 (1978).

22. F. T. S. Yu and P. H. Ruterbusch, Opt. Laser Tech., 14, 273 (1982).

23. G. Gerhart, P. H. Ruterbusch, and F. T. S. Yu, Appl. Opt., 20, 3085 (1981).

IX. Personal

       Francis T. S. Yu   Principal Investigator
       G. Gheen   Research Assistant
       N. H. Wang   Research Assistant

X. List of Publications

1.   F. T. S. Yu, S. L. Zhuang and N. H. Wang, "IC
      Chip Inspection with Incoherent Optical Pro-
      cessing," SPIE Proceedings on Sensor Robot
      Technology," San Diego, August 1982.

2.   F. T. S. Yu, G. Gheen and N. Wang, "Construction
      of a Two-Dimensional Color Hologram with the use
      of Source Encoding Technique," to be submitted to Optics
      and Laser Technology.

3.   F. T. S. Yu and G. Gheen, "White-Light Image
      Subtraction," in preparation.

END

DATE
FILMED

7-85

DTIC